Urban Climate 23 (2018) 260–286

Contents lists available at ScienceDirect

Urban Climate

journal homepage: http://www.elsevier.com/locate/uclim

Evaluating the impacts of greening scenarios on thermal comfort and energy and water consumptions for adapting Paris city to climate change

C. de Munck[a,*], A. Lemonsu[a], V. Masson[a], J. Le Bras[a], M. Bonhomme[b]

[a] Centre National de Recherches Météorologiques, GAME, Météo-France/CNRS, Toulouse, France
[b] Laboratoire de Recherche en Architecture, Toulouse, France

ARTICLE INFO

Article history:
Received 31 May 2016
Received in revised form 29 November 2016
Accepted 5 January 2017
Available online xxxx

Keywords:
Climate change adaptation
Greening strategies
Thermal comfort
Energy consumption
Water resources

ABSTRACT

Recent climate projections predict an amplification of global warming and more frequent extreme events such as heat waves. Therefore, the adaptation of cities to counterbalance these adverse changes is urgent. Among available adaptation strategies, urban greening is a measure that is frequently encouraged to improve thermal comfort or energy demand, but whose impacts are not well known at the scale of cities. In this study we evaluate the effects of various urban greening scenarios based on urban climate simulations across the Paris area. The modelling relies on the Town Energy Balance model. The scenarios tested consist of an increase in ground-based vegetation or an implementation of green roofs on compatible buildings, or the two combined. Results show that increasing the ground cover has a stronger cooling impact than implementing green roofs on street temperatures, and even more so when the greening rate and the proportion of trees are important. Green roofs are however the most effective way to reduce energy consumption, not only in summer but also on an annual basis. The effects the various greening measures may have over different seasons is finally addressed in order to draw up a comprehensive inventory of the climatic impacts of such strategies.

© 2017 Elsevier B.V. All rights reserved.

1. Introduction

Current climate projections forecast an amplification of the global warming (Meehl and Tebaldi, 2004; Stocker et al., 2013) and an increase in extreme events (Giorgi, 2006). Those global trends that translate at regional and local scales, are likely to have significant impacts in cities, that are home to the majority of the population, namely a change in the intensity of the urban heat island (highly dependent on the soil water resources, such as highlighted by the work of Lemonsu et al., 2013), increased health risks (as attested by the 15,000 excess deaths due to extreme heat observed in August 2003, Hémon and Jougla, 2004), not to mention the increase in the use of air conditioning to meet the comfort needs of the inhabitants (180% between 2003 and 2020 according to Adnot, 2003a,b) . These perspectives make cities territories where not only mitigation issues will be the strongest, but also potentially territories more vulnerable to climate change than natural environments.

* Corresponding author.
E-mail address: cecile.demunck@gmail.com (C. Munck).

http://dx.doi.org/10.1016/j.uclim.2017.01.003
2212-0955/© 2017 Elsevier B.V. All rights reserved.

There are different forms of adaptation strategies to reduce this urban vulnerability, involving actions on requalification of surfaces, urban forms, inner and outer building envelopes, or on individual behaviors. Urban greening strategies, more specifically, have multiple interests. Thanks to vegetation cooling potential, they are both adaptation measures to climate change and mitigation measures for urban heat island and air-conditioning demand. Beyond climatic considerations, urban greening also delivers additional benefits to the urban ecosystem, such as a better management of stormwater (Ashley et al., 2011; Stovin, 2010; Stovin et al., 2008), a reduction of air pollution (Currie and Bass, 2008; Hill, 1971; Nowak et al., 2006; Pugh et al., 2012) or an increase in urban biodiversity (Getter and Rowe, 2006; Madre et al., 2014; Mullaney et al., 2015) for example.

This is by modifying its radiative, thermal, hydrological and aerodynamic properties that vegetation affects the urban environment. These modifications result from three physical processes: direct evaporation of the water held in the soil and intercepted by the foliage of plants (daytime and nighttime), the transpiration of all types of plants (generally daytime, but can also occur at nighttime for some plant species or under certain climates), and finally the interception of solar radiation for tree species (daytime). But there is a wide range of greening solutions that have different effects depending on the scale at which they are implemented (building, street, neighbourhood, city), on the plant species selected, on the local climatic conditions, but also on the aspects studied (thermal comfort, energetics, dynamics, hydrology, etc.). This is shown by the vast literature on the subject, whether from experimental or numerical studies.

Greening the building envelopes can reduce surface temperatures compared to artificial surfaces, which limits the amount of heat that can penetrate into buildings (Eumorfopoulou and Kontoleon, 2009; Kontoleon and Eumorfopoulou, 2010; Onmura et al., 2001; Sternberg et al., 2011; Takebayashi and Moriyama, 2007; Wong et al., 2010). In doing so, they diminish the seasonal temperature variations inside buildings (Castleton et al., 2010), generating energy savings, but without totally achieving the efficiency of conventional insulation according to Eumorfopoulou and Aravantinos (1998) and Eumorfopoulou and Kontoleon (2009). Urban greening takes also other forms through street trees, urban parks or forests. On the basis of a meta-analysis of the literature on these types of strategies, Bowler et al. (2010) show that urban parks generate an average day cooling in the range of 0.94 °C, with variations which are explained in particular by the size of the park (Barradas, 1991; Chang et al., 2007) and its composition (tree/lawn ratio, Potchter et al., 2006) but also the surrounding climate. They also highlight that the temperatures under the trees are systematically cooler than the surroundings during the day, with variations depending on tree shading capacity Shashua-Bar and Hoffman (2000). At nighttime, however, tree canopy could retain heat (Liangmei et al., 2008; Souch and Souch, 1993; Taha et al., 1991). Besides, a study by Souch and Souch (1993) suggests that the thermal performance of trees can vary depending on the type of surface on which they are planted (grass or concrete, for example). The evapotranspiration potential conditioned to water status of plants and soils, and irrigation practices, is also a crucial point which has received very little attention to date, except by Shashua-Bar et al. (2009) who propose an efficiency coefficient which links cooling effect and evaporation.

For operational purposes within the frameworks of urban policies, the analysis and evaluation of such strategies need to be examined at a large scale. So far, only a few numerical studies investigate the cooling potential of large-scale strategies of urban planning, such as the implementation of green and blue corridors for Paris urban area (Groupe Descartes, 2009), or of green roofs over Toronto (Bass et al., 2003) and New York City (Rosenzweig et al., 2009).

Our study aims to complement the scientific literature, but also better meet the expectations of urban planners and decision makers, through a physically-based and detailed modelling of urban climate, using Paris urban area as a study case. The originality of the work lies (1) in the development of realistic urban greening scenarios, implemented locally but assessed at city scale; (2) in the comparison of different vegetation installations in urban environment, on roofs (with or without irrigation) and on the ground (lawns, mixed vegetation); (3) in the multi-criteria evaluation of scenarios which covers the issues of heat exposure and thermal comfort, energy consumption, and water demand; and (4) in the time scales that are investigated (for a specific heat wave, as well as at seasonal and annual scales).

The next section (Section 2) presents the basis for the construction of the different scenarios that we simulated, the numerical configuration used as well as its evaluation before greening. Then various impacts are assessed, both in extreme summer conditions (heat wave, Section 3) and for the rest of the year (Section 4) to evaluate whether these greening measures devised to meet heat wave issues have adverse effects on the rest of the year or not. The impacts studied are thermal comfort and energy consumption for use of air-conditioning (AC) and heating, which are good indicators of the vulnerability of cities to heat waves, but are also about the management of urban water (volumes required for watering the vegetation and generated by surface runoff throughout the year). The last section (Section 5) draws the conclusions of this work and suggests ways to develop this approach.

2. Methodology for evaluating greening scenarios at city-scale

The initial aim of this study is to evaluate, based on modelling, greening scenarios which may represent strategies to improve future summer conditions in cities. As the European heat wave of 2003 is identified by the scientific community to be representative in mean temperatures of summers of the second half of the 21st century (Déqué, personal communication), the meteorological conditions associated to this heat wave are taken as a study case to evaluate greening scenarios. This methodology, focusing on Paris city, relies on simulating the urban climate of Paris with the Town Energy Balance (TEB) urban canopy model (Hamdi and Masson, 2008; Masson, 2000). The first step consists in designing for Paris city greening scenarios that are at the same time realistic and promising and that can also be taken into account by our model. In a second step, the urban climate of Paris is simulated at the spatial resolution of 1 km with TEB in offline mode (with meteorological forcings) for each

greening scenario, alongside sustainable strategies for energy and water usage. This is done under a 10-year meteorological forcing (1999–2008) that includes the heat wave event of 2003 (8–13 August 2003). This way both can be studied the benefits of greening scenarios in a heat wave context as well as their respective impacts at the scale of other seasons. This methodology allows for a comprehensive assessment of greening strategies to be realised. During the simulations, indicators identified to be representative of city vulnerability to climate change are computed so that the impacts of the respective scenarios can be quantified and compared.

2.1. Simulation configuration and evaluation of the reference simulation

2.1.1. Simulation configuration

For this study, the simulations were performed with the SURFEX surface scheme (Masson et al., 2013), and more specifically with TEB, the Town Energy Balance model (Hamdi and Masson, 2008; Masson, 2000) built in SURFEX for urban and artificial surfaces, and ISBA, the Interaction between Soil-Biosphere-Atmosphere model (Boone, 2000; Noilhan and Mahfouf, 1996) for natural surfaces (soil and vegetation). The configuration chosen for the simulation follows that set up in the MUSCADE project (Masson et al., 2014b), which this study is part of. This configuration is detailed in Appendix A. In this configuration that involves a platform of models, the input data for SURFEX are provided by an architectural model, the GENerator of Interactive Urban blockS (GENIUS, Bonhomme, 2013; Bonhomme et al., 2013). This model provides SURFEX with land cover information at the resolution of 250 m (including existing urban green spaces), and more specifically provides TEB with a map describing urban morphology based on eight types of urban blocks (Continuous pavilion, Discontinuous pavilion, Continuous block, Discontinuous block, High-rise tower, Ancient centre, Industrial building) with specific geometric features and building dates. Then, TEB translates these eight urban blocks into five building types (Haussmannian building, Individual housing, Dense collective housing, Office tower, Warehouse) and aggregates them at the resolution of 1 km to reduce computational costs. Five types of building use (Residential, Office, Industrial, Agricultural, Commercial) complete this representation. The radiative and thermal characteristics of buildings are prescribed on the basis of building type and age (characteristics provided in Appendix A), building equipment characteristics (air-conditioning, heating, ventilation) on the basis of building use (see Appendix A) and scenario hypothesis. For example, in our simulations, virtuous temperature set points for air-conditioning and heating are chosen to be in line with the sustainability of the greening scenarios: 19°C for heating and 26°C for air-conditioning. Heating and air-conditioning are active all-year round and triggered as soon as their respective temperature set points are reached whatever the season.

In this configuration TEB is run in offline mode (i.e. with 1D meteorological forcings as opposed to coupled to an atmospheric model), at the spatial resolution of 1 km, and with most of its parameterizations activated to allow for more physical processes and interactions to be accounted for: vertical turbulent diffusion within multilayer urban canyons (Hamdi and Masson, 2008; Masson and Seity, 2009), building energetics (Bueno et al., 2012; Pigeon et al., 2014), urban vegetation on the ground (Lemonsu et al., 2012), greenroofs (de Munck et al., 2013a), as well as a module for computing thermal comfort indexes (Fiala et al., 2012; Pigeon, 2011). In addition, the urban weather generator (UWG) implemented in SURFEX is applied in order to derive a 2D temperature forcing from a 1D forcing and city features (Le Bras and Masson, 2015). Despite efforts to improve the model, some physical processes are not yet represented in the version used in this study, such as the shading effect of trees, as well as the radiative trapping by tree canopies.

Under this configuration, the modifications to the surface induced by the ground greening scenarios translate within TEB into the modification of the respective fractions of roads and green spaces, wherever greening is possible and according to the three greening ratios tested. In the case of scenarios with roof greening, the thermal and radiative characteristics of the greened artificial roofs (those of warehouses and individual and dense collective buildings) are replaced by those of green roofs. The total density of urban vegetation induced by the different scenarios is presented in Fig. 1. Additional surface characteristics (building fraction and type, usage and height of buildings) which may be helpful for the analysis of simulation results are provided in Appendix A.

2.1.2. Evaluation of the reference simulation

The reference simulation, which takes into account the existing urban vegetation and is therefore the closest to reality in terms of land cover, is evaluated to appreciate the performance of the model configuration set up in this study, both during the heat wave (8–13 August 2003) and the decade (1999–2008) studied. This evaluation exercise is based on the 2-m air temperatures recorded at eight operational weather stations that are located within the spatial domain studied (see Appendix B). They provide complete series of daily minimum and maximum temperatures over the 10-year period 1999–2008, and hourly temperatures during the six days of the 2003 heat wave are also available for seven of them. At a 1-km horizontal resolution, the model cannot accurately reproduce the sub-grid heterogeneity in the surface characteristics. Therefore it is more suitable to compare model estimates and observations for groups of stations having similar surface characteristics rather than to conduct a mesh by mesh comparison. Consequently, the evaluation exercise is performed for two types of stations, those *urban* and those *rural* (see Appendix B), depending on the urbanised fraction of the model mesh they belong to, on average $81 \pm 16\%$ and $21 \pm 16\%$ respectively. While simulated and observed hourly temperatures are compared for the 2003 heat wave, minimum and maximum temperatures are compared in terms of the monthly climatology over the 10-year period studied. Appendix B provides graphs showing the evolution of simulated and observed 2-m temperatures during the heat wave as well as that of monthly means of simulated and observed 2-m minimum and maximum temperatures (referred to thereafter as TN mean and TX mean). The associated statistical scores are summarized in Table 1.

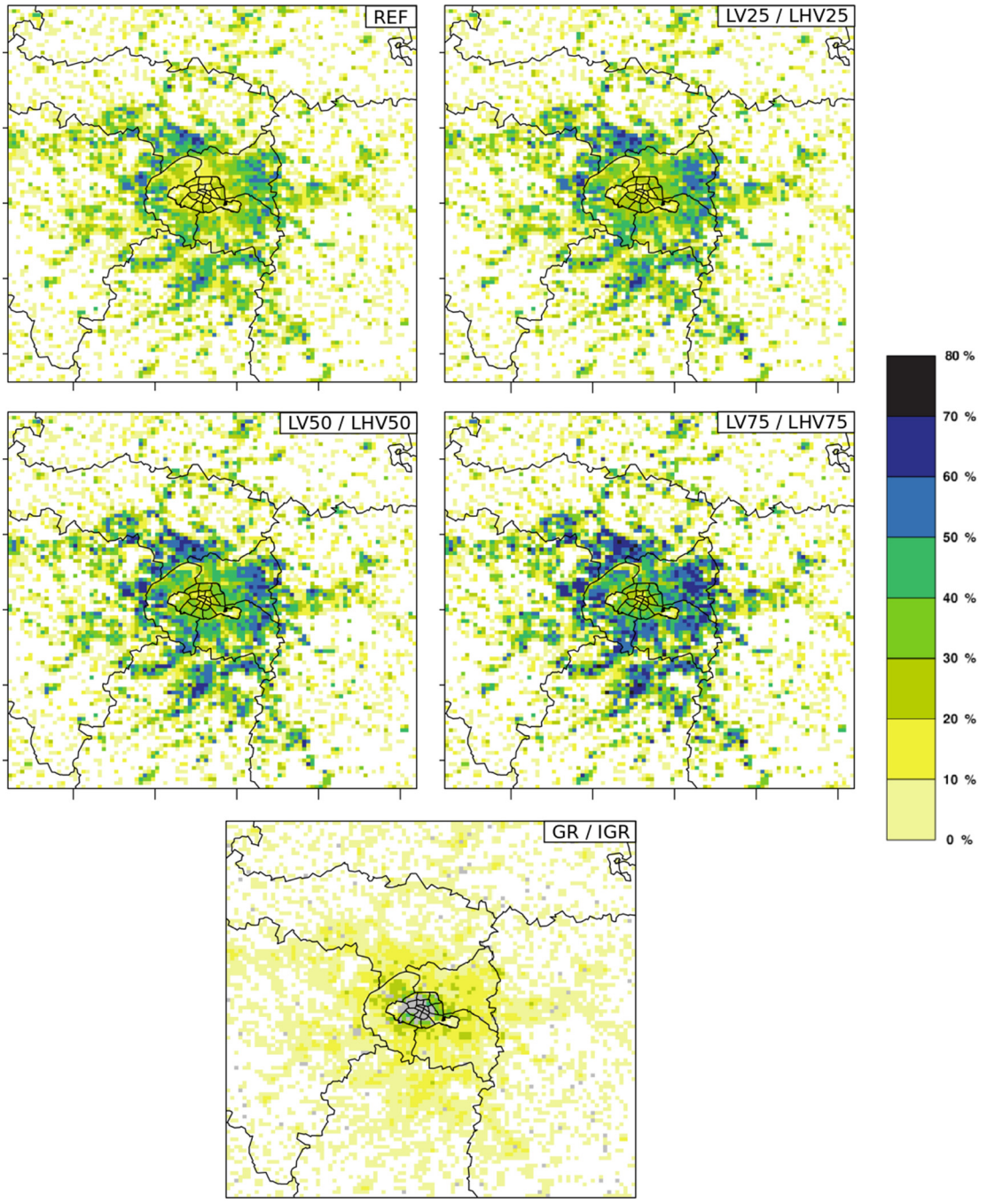

Fig. 1. Urban vegetation density in each 1-km^2 grid mesh. Represents ground vegetation for LV25, LHV25, LV50, LHV50, LV75, and LHV75 scenarios, and rooftop vegetation for GR and IGR scenarios (grey squares show the location of buildings without green roof, i.e. Haussmannian buildings and office buildings).

During the heat wave, although the model correctly simulates the daily dynamics of temperatures (see Appendix B), the bias values obtained ($+1.33$°C for urban stations and $+1.14$°C for rural ones) suggest that the model tends to simulate temperatures a little higher than those observed, whatever the location of the station. With standard deviations for simulated temperatures very close to those observed at stations, 5.22°C versus 5.06°C respectively at urban stations and 6.03°C versus 5.51°C at rural stations, the model is capable of capturing the slightly higher temperature variability observed at rural stations. Running at the spatial resolution of 1 km, an average error on the six days of the heat wave of about 1.9°C is made on the simulated temperatures, whether in urban or rural areas. This error seems to be due to an overestimation by the model of the temperatures

Table 1
Root mean square errors (RMSE) and mean bias errors (MBE Model-Obs) associated with 2-m air temperature for the reference simulation during the 2003 heat wave and for the mean climatology of the 1999–2008 decade.

	8–13 August 2003		1999–2008 decade			
	T (hourly)		TN mean		TX mean	
	Urban	Rural	Urban	Rural	Urban	Rural
RMSE (°C)	1.93	1.90	1.26	0.77	0.73	0.86
MBE (°C)	+1.33	+1.14	+1.25	+0.76	+0.53	+0.71

during the first three days of the heat wave (see Appendix B), which is probably the consequence of an insufficient representation of advection processes in the simulation configuration used (discussed further in Appendix B).

On average over the decade simulated, RMSE and MBE values obtained show that at the spatial resolution of 1 km, be it at night or during the day, the model configuration we use tend to overestimate 2-m air temperatures. At night, the model present a RMSE of 1.26°C and a MBE of +1.25°C for urban stations and a RMSE of 0.77°C and a MBE of +0.76°C for rural stations. Whatever the season, errors on the TN mean are lower for rural than for urban stations (on average by 0.5°C for both scores), suggesting that the model further overestimates temperatures at night in urban settings. This tendency of the model to overestimate 2-m temperatures is much less pronounced at daytime than nighttime, with RMSE and MBE values two times less those at night (RMSE of 0.73°C and MBE of +0.53°C). Contrary to nighttime period, the model presents a slight tendency to overestimate more maximum temperatures for rural than for urban stations during the day. As far as temperature variability is concerned, the calculation of the standard deviations for the monthly climatology showed that they do not differ much between urban and rural stations: for the TN mean, they are on average 4.77°C for observations and 4.63°C for model estimations, and for the TX mean respectively 6.79°C and 6.48°C. Such standard deviation values that are equivalent to slightly less than for observations demonstrate that the model is quite good at capturing the variability found in the observations for the decade studied.

Our results are in line with previous numerical studies running with the TEB model that are based on more sophisticated simulation configurations than the one used in our study. When simulating the same six-day period of the 2003 heat wave with the TEB model coupled to a mesoscale atmospheric model, de Munck et al. (2013b) obtain at the spatial resolution of 1.25 km a similar MBE (+1.0°C) and a higher RMSE (2.6°C) values than those obtained with our simulation configuration for the prediction of 2-m temperatures. It's only by running at a higher spatial resolution (250 m) and with a very detailed description of surface characteristics that the performance of the model is improved, with a MBE of +0.2°C and a RMSE of 1.5°C, yet comparable to the one obtained with our simulation configuration. Similar scores are obtained by Lemonsu et al. (2015) who simulate the 2003 heat wave at the spatial resolution of 1 km with a chain of models including TEB: a MBE on nighttime temperatures ranging from +0.41 to +3.72°C between the most and the least urbanised land covers, with errors ranging from 0.83 to 3.83°C, and at daytime, an average MBE of −0.52°C and errors ranging from 0.78 to 2.06°C. In order to minimize the impact of the biases and errors highlighted in the reference simulation, the analysis of the impacts of the greening scenarios in the present study is carried out in relative terms (relative to the reference simulation before greening).

2.2. Designing realistic greening scenarios for Paris city

The greening strategies we evaluate consist in greening the city wherever possible by partially transforming artificial urban surfaces available into green spaces. We assume as partly available for greening, the urban surfaces at ground level such as pavements, squares, roundabouts and car parks (surfaces that are neither built as buildings or roads, or already vegetated), as well as the roofs of some building types. At ground level, a certain percentage of the urban surface available for greening

Table 2
Characteristics of the scenarios simulated.

Scenario acronym	Conversion to vegetation	Additional green areas (km^2)	Vegetation type	Irrigation
GR	Roofs of suitable buildings[a]	251 (+28%)	Sedums	No irrigation
IGR	Roofs of suitable buildings[a]	251 (+28%)	Sedums	Drip irrigation
LV25	25% of ground available[b]	100 (+11%)	Low vegetation: grass and small shrubs	Sprinkler systems
LV50	50% of ground available[b]	199 (+23%)		
LV75	75% of ground available[b]	298 (+34%)		
LHV25	25% of ground available[b]	100 (+11%)	Low and high vegetation: 60% grass and small shrubs 40% of deciduous trees	Sprinkler systems
LHV50	50% of ground available[b]	199 (+23%)		
LHV75	75% of ground available[b]	298 (+34%)		
LHV75-IGR	75% of ground available[b]	549 (+62%)	Low and high vegetation	Sprinkler systems
	Roofs of suitable buildings[a]		Sedums	Drip irrigation

[a] "Suitable buildings" for the implementation of extensive green roofs refer to building types with flat roofs for which the energetical performance has been demonstrated in the literature, i.e. individual and dense housing and warehouses.

[b] "Ground available" refers to ground surfaces which are neither natural, nor built as buildings or roads. In a real city it corresponds to pavements, car parks, squares, roundabouts, etc.

is converted to green space, either 25, or 50, or 75%. This greening is realised with either low vegetation (grass and small shrubs) or a mix of low and high (10 m) vegetation composed of 40% of deciduous trees (often referred to hereafter as *mixed wooded vegetation*). At roof level, the surfaces available for greening are those of roofs of low-rise buildings (following the conclusions of Ng et al., 2012) for which architecture or regulation would allow for their installation, which means in TEB, roofs of Individual and Dense collective buildings and Warehouses (see Appendix A). Roofs of Haussmannian buildings are excluded for architectural and regulatory reasons and roofs of office towers for their inefficiency. On the roofs of the three types of suitable buildings are implemented extensive green roofs (planted with sedum), which are recognized for their energetical performance. The characteristics simulated in TEB for this type of green roof are described in de Munck et al. (2013a). Following previous studies highlighting that vegetation is an effective adaptation measure only if it is watered (Daniel et al., 2016; Kounkou-Arnaud et al., 2013), we chose to water ground vegetation in summer whatever the scenario. In the case of green roofs two scenarios are tested, with or without irrigation in summer. A last scenario, consisting in combining implementation of irrigated green roofs and greening of 75% with a mixed wooded vegetation is also simulated.

For summer irrigation, the choice of watering volume and schedule is based on a sensitivity analysis undertaken with TEB under the meteorological conditions of the 2003 heat wave (de Munck, 2013), which aim was to optimize plant water use for a non-restricted evapotranspiration, hence air cooling effect. With regard to volumes, we chose for green roofs 25 L per m^2 per week, a value derived after the guidelines provided by SOPREMA (international manufacturer specialized in waterproofing solutions for urban infrastructures including green roofs and walls, SOPREMA, 2011) for France and in drought conditions. For ground vegetation, we tested three volumes (25, 50 and 75 L per m^2 per week), as well as three watering schedules (in 3, 6 or 8 h), all three at night, in order to optimize both plant water use and the nighttime air cooling effect. Night-time watering was chosen to improve night's rest and reduce nighttime thermal stress, a major factor related to excess mortality during the 2003 heat wave in France (Dousset et al., 2011; Ledrans et al., 2005). We concluded that a unique watering schedule, over eight hours between 21:00 and 05:00 local time, providing the equivalent of 25 L m^{-2} $week^{-1}$ (i.e. 4 10^{-5} kg of water m^{-2} s^{-1}) would be suitable for both ground and roof vegetation, the only difference being the watering system, with sprinklers for ground vegetation and drip irrigation for green roofs. The watering with sprinklers is parameterized in TEB as rain, which is realistic for low vegetation but may slightly overestimate the amounts of water intercepted in the case of trees.

For practical reasons, acronyms were given to those scenarios. They are provided in Table 2 alongside a summary of their characteristics, and used thereafter. In all cases, scenarios increased the density of existing urban vegetation (represented by the REF scenario) in the proportions which are provided in Table 2 and illustrated by the maps of Fig. 1. Over the entire simulation domain, greening 25, 50 of 75% of available ground-based urban surfaces corresponds to increasing existing green space density by respectively 11, 23 and 34%. Also, as can be seen on Fig. 1, because the ground surface available for greening is quite low in the city centre, the more we green the ground (from 25 to 75%), the more the greening is only possible on the outskirts of Paris. On the contrary greening suitable roofs (GR and IGR scenarios) allows within Paris to compensate for the lack of ground space. The increase in urban vegetation density obtained through these two scenarios is far from negligible at the scale of the simulation domain (+28%) and is higher locally within Paris city (between +30 to +40%). The scenario combining the greening of both ground and roofs (LHV75-IGR) presents the maximum vegetation density increase with +62%.

2.3. Choice of indicators

The impacts of greening strategies are analyzed by comparing three types of indicators of interest which are computed by TEB: levels of thermal heat stress reached, energy consumptions for cooling and heating buildings, water resources required for summer watering as well as urban surface runoff (from artificial and natural urban surfaces) all year round.

The 2-m air temperature is compared between scenarios as a first indicator of greening impact. Then levels of thermal comfort or heat stress (and time spent at each level) are evaluated through the Universal Thermal Climate Index (UTCI, Fiala et al., 2012) and the thresholds established by the Glossary of Terms for Thermal Physiology (The Commission for Thermal Physiology of the International Union of Physiological Sciences, 2003) and indicated in Table 3. The UTCI is calculated in TEB taking into account the climatic conditions for a person placed in the middle of the urban canyon (air temperature and humidity, wind speed, direct and reflected solar radiation and infrared solar radiation emitted by the walls of the canyon). The UTCI can be calculated for a person who stands in the sun or in the shade. In the latter case, the calculation of the UTCI will not take into account the direct solar radiation.

To compare the energetical performances of the greening scenarios in the context of the 2003 heat wave, we choose for indicators the energy consumption cumulated as well as the peak of energy demand during the heat wave (air-conditioning).

Table 3
Assessment scale of UTCI for high temperatures. Source: www.utci.org.

UTCI (°C)	Thermal stress level
Above +46	Extreme heat stress (EXS)
+38 to +46	Very strong heat stress (VSHS)
+32 to +38	Strong heat stress (SHS)
+26 to +32	Moderate heat stress (MHS)
+9 to +26	Thermal comfort

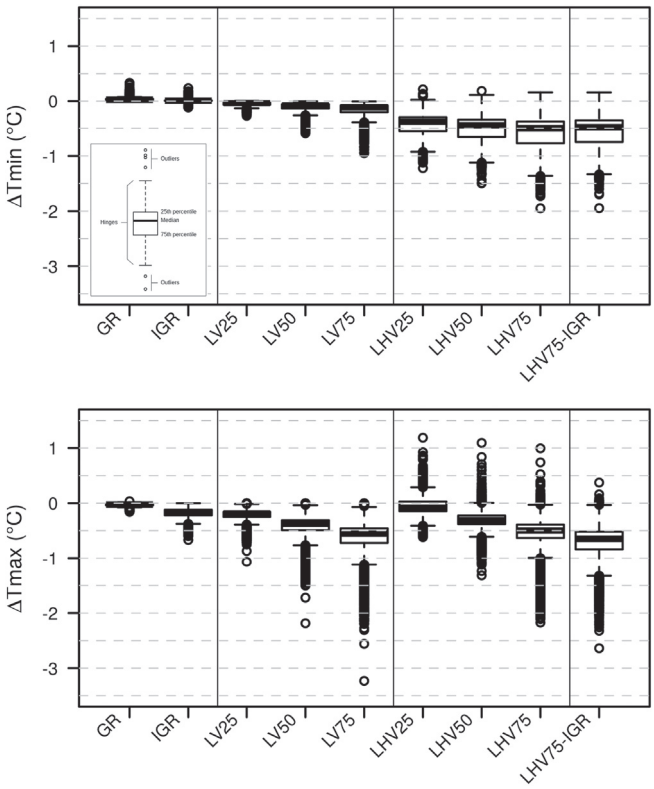

Fig. 2. Boxplots of average impacts of greening scenarios on minimum and maximum daily urban 2m-temperatures over the entire simulation domain during the 2003 heat wave for each scenario and compared to the simulation before greening (REF).

For the seasonal analysis, we compare the 10-year mean energy consumption cumulated during each of the four seasons (air-conditioning and heating).

3. Impacts in the context of heatwave

The impacts of greening scenarios are estimated for the heat wave of August 2003, and more specifically for a six-day period, extending from the 8th to the 13th of August, chosen to be the hottest period of this exceptional heat wave for the region Ile-de-France. These six days were marked by settled anticyclonic conditions, with dry and stable air masses in the lower layers of the atmosphere, which got warmer and warmer until the 14th of August, marking the end of the heat wave.

3.1. Thermal impacts

3.1.1. 2-m air temperatures

To have in mind the order of magnitudes between the impacts of greening strategies in terms of 2-m air temperatures and the indicators presented previously, we compared the minimum and maximum 2-m air temperatures through the analysis of the temperature anomalies between each greening scenario and the simulation before greening (named REF).

Based on our simulations, our results (Figs. 2, 3 and 4) suggest that greening suitable roofs does not have an impact on 2-m air temperatures unless those are irrigated and that this impact only really appears at daytime. And even in this case, the average daytime cooling induced during the six days of the heat wave at the scale of the entire simulation domain is relatively limited, with a median cooling of −0.17°C (Fig. 2). Looking at the spatial distribution of this cooling, the potential of irrigated green roofs for cooling maximum temperatures generally ranges from −0.25 to −0.5°C depending on building type, respectively for individual and dense collective housing. It is noticeable even in the centre of Paris and can reach up to −0.67°C locally (Fig. 4). The maximum cooling induced by irrigated greenroofs in the simulation domain in the course of the heat wave is −0.97°C.

The temperature anomalies generated by the increase in ground vegetation (systematically watered) are shown on Fig. 2. These scenarios show, as expected, a greater cooling of 2-m temperatures than that generated by roof level vegetation with three significant results:

1. For a given type of vegetation (LV or LHV) night and daytime cooling do not have the same magnitude (Fig. 2). A maximum effect is observed at daytime for scenarios with the addition of low vegetation, with a median cooling of −0.19°C, −0.37°C

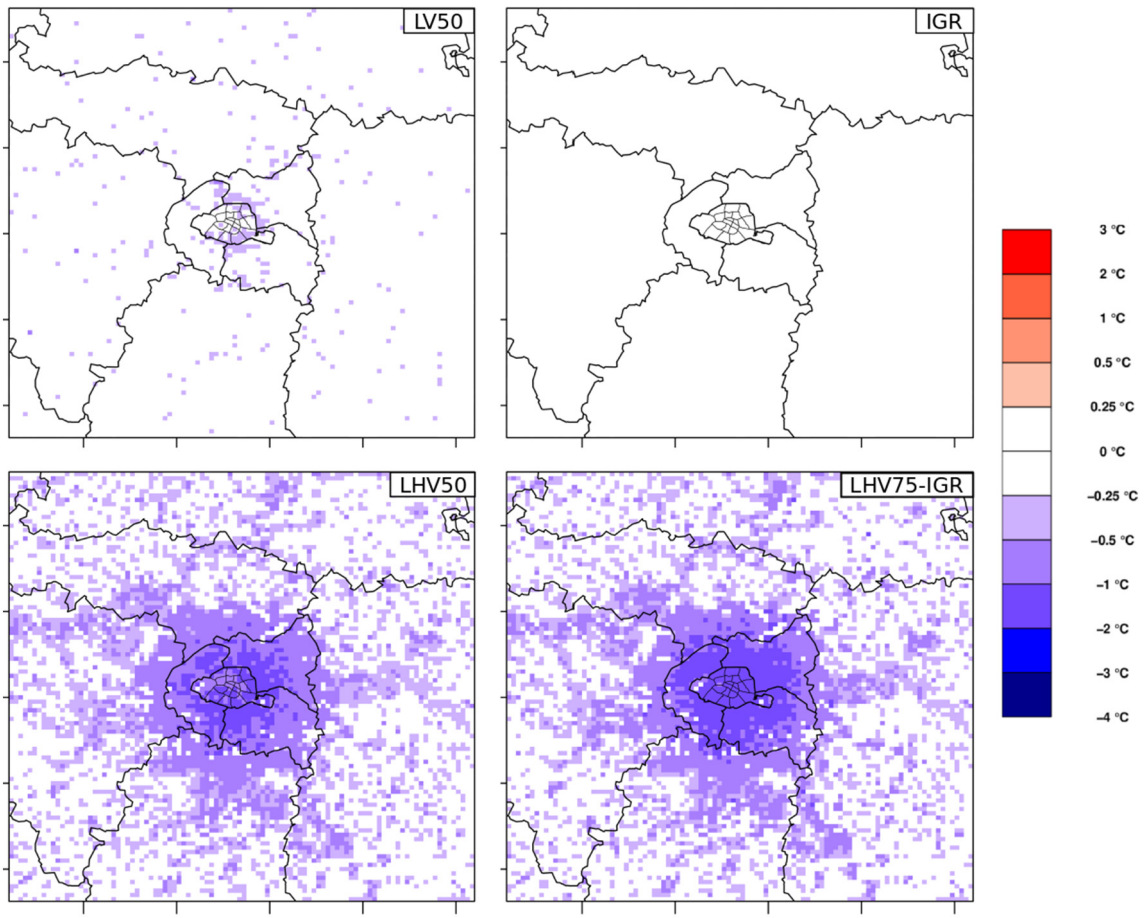

Fig. 3. Spatial distribution of the impacts of greening over **minimum daily urban 2m-temperatures** for intermediate ground greening (LV50 and LHV50), roof greening (IGR) and maximum greening (LHV75-IGR), expressed as the average impacts during the six days of the heat wave.

and −0.55°C respectively for LV25, LV50 and LV75 (Fig. 2). Conversely, the implementation of a mixed wooded vegetation leads to a maximum effect at nighttime, with a median cooling of −0.38°C, −0.45°C and −0.50°C respectively for LV25, LV50 and LV75 (Fig. 2). While it is logical for the cooling effect to be optimum at daytime when the vegetation is photosynthetically active (and therefore evapotranspiration rates at their maximum), as is the case for low vegetation scenarios, we obtain a higher cooling potential at night for the mixed wooded vegetation scenarios that is explained by the watering schedule and the vegetation type. Indeed, when the trees are watered at night, sprinklers being simulated in TEB as artificial rain, a large part of the water intercepted by the foliage and the soil is directly evaporated and is no longer available during the day, generating less cooling at that time of day. This occurs also for low vegetation, but to a lesser extent due to its smaller interception surfaces and lower transfer turbulent coefficients. Note that for trees, this phenomenon is probably more pronounced than in reality due to sprinkler watering since greater amounts of water are intercepted by tree leaves and are directly evaporated, hence are not stored in the ground. This shows the limits of the current parametrization for the watering of ground vegetation (that was due to constraints in the code structure of the ISBA scheme), which is undifferentiated for grasses and trees. These timing and magnitude differences in the cooling generated by low and mixed wooded vegetation scenarios are well visible on the maps of Figs. 3 and 4 when comparing LV50 and LHV50 scenarios. During the night, the strongest cooling is generated by the LHV50 scenario and ranges on average during the heat wave between −0.25 and −2°C, with a maximum cooling potential observed in areas of dense collective housing. Meanwhile, the LV50 scenario only generated a cooling of around −0.25 to −0.5°C. In the course of the heat wave, the greatest cooling of minimum temperatures generated by the LVH50 and LV50 scenarios amounts respectively to −2.2 and −1.1°C.

2. When looking at each type of ground vegetation simulated separately, the higher the surface greening rate, the greater the cooling generated. When greening 25, 50 or 75% of available surfaces with low vegetation, this corresponds to a daytime cooling of −0.19, −0.37 and −0.55°C and a nighttime cooling of −0.04, −0.08 and −0.12°C (median values of boxplots on Fig. 2). Similarly, for a mixed vegetation, this corresponds to a daytime cooling of −0.08, −0.31 and −0.49°C and a nighttime cooling of −0.38, −0.45 and −0.50°C. Looking locally, if taking LV scenarios as an example, the greatest

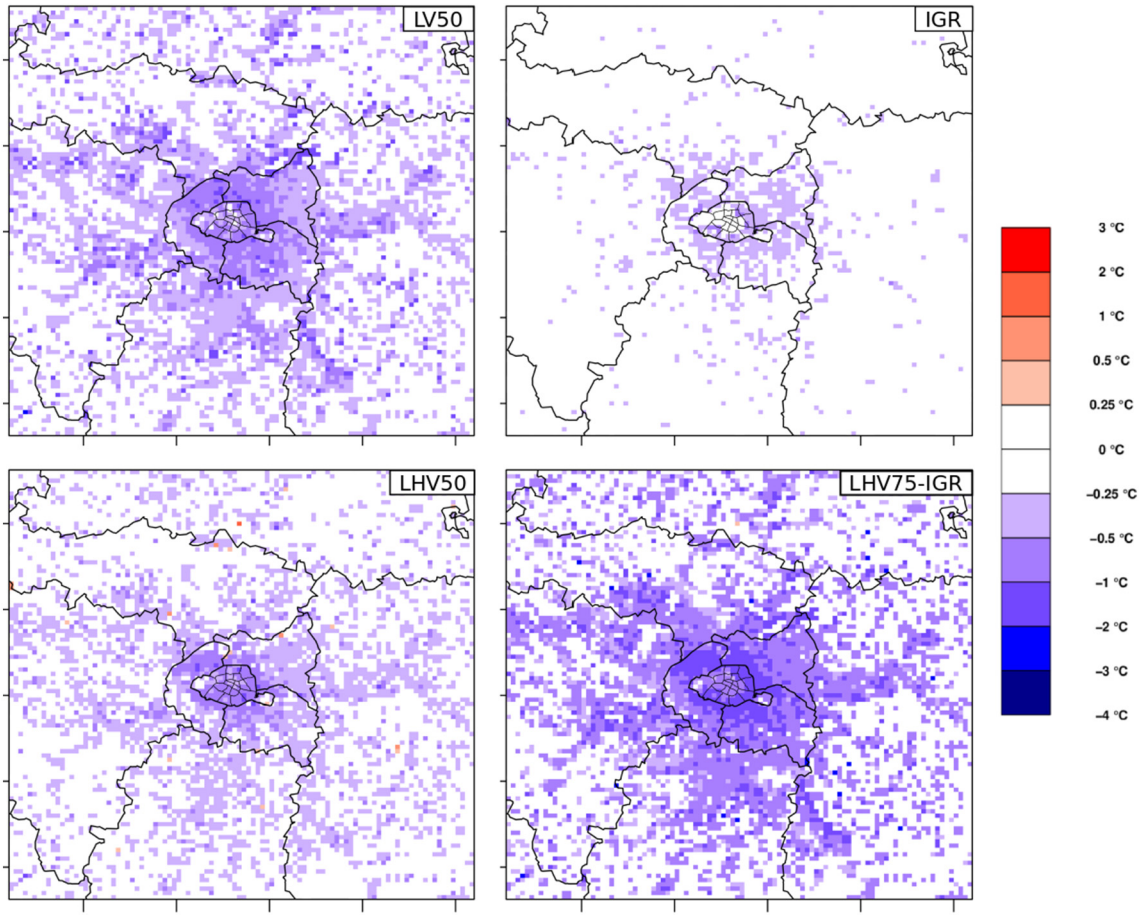

Fig. 4. Spatial distribution of the impacts of greening over **maximum daily urban 2m-temperatures** for intermediate ground greening (LV50 and LHV50), roof greening (IGR) and maximum greening (LHV75-IGR), expressed as the average impacts during the six days of the heat wave.

reduction in maximum temperatures estimated at the scale of the simulation domain amounts to about −0.5°C for LV25, −1°C for LV50 and −2°C for LV75.

3. Nighttime results suggest that for similar ground surface greening rates, the cooling potential of a mixed vegetation composed of 40% of trees is more effective than that of a vegetation composed only of grasses and small shrubs. For the time being it is harder to draw conclusions from daytime results since the model does not yet account for tree shading effects.

As for the maximum greening scenario combining LHV75 and IGR hypothesis, its impact on 2-m temperatures is quite similar to that of the LHV75 since the cooling potential of IGR on street level temperatures is limited (Fig. 2). It is only performing sensibly better at daytime in areas around Paris city centre with dense collective housing where IGR manage to further enhance the cooling, resulting in a domain median impact of −0.65 °C.

3.1.2. UHI intensity

Along the cross-section defined on the map of Fig. 5, the 2-m nighttime UHI intensity between Paris city centre and the 50-m away countryside was estimated before greening at around 5°C with the standard spatial structure represented by the grey line. As expected from previous temperature results, the greening of roofs does not modify the UHI intensity at all since IGR and REF temperature profiles are identical. To evaluate the maximum impact of urban ground greening on the UHI, previous temperature profiles were compared to the scenarios with the greatest greening rate (75%, i.e. LV75, LHV75 and LHV75-IGR). As expected from previous results, the scenario with a mixed wooded vegetation (LHV75) induced the greatest reduction in UHI intensity (−1.2°C), which lowers the UHI to 3.8°C. The impact of low vegetation on UHI is relatively low in comparison (in the range of 0.25°C). As for irrigated green roofs, they do not allow for a further reduction of the UHI intensity induced by greening the grounds (LHV75-IGR).

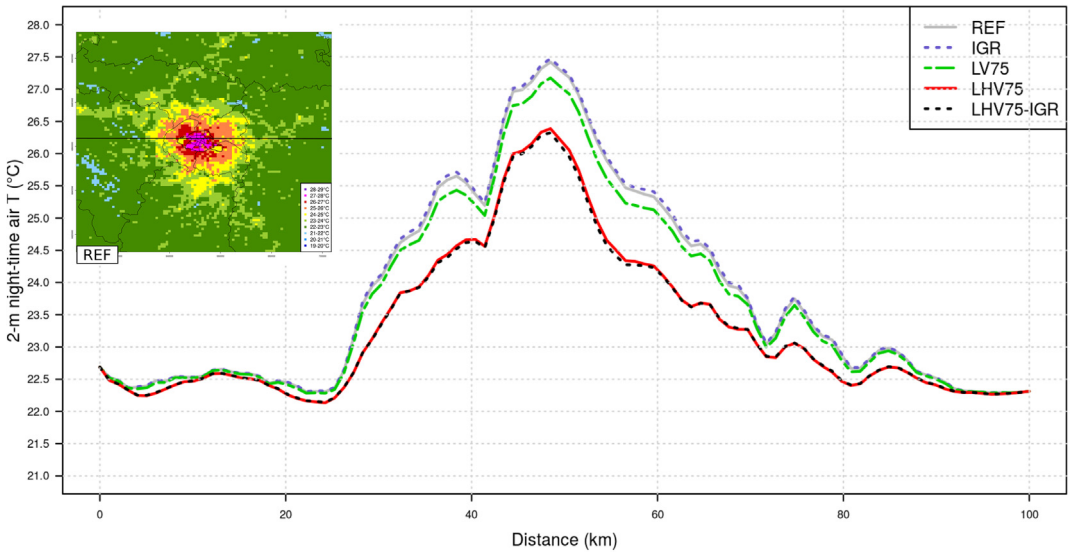

Fig. 5. 2-m mean nighttime air temperature profiles during the six days of the heat wave for the west-to-east cross section identified on the map of temperatures presented for the REF simulation, estimated across three hourly terms - 2, 3 and 4 UTC. The profile for the baseline simulation (REF) shows a heat island intensity of around 5°C.

3.1.3. Thermal comfort

To analyze the respective impacts of the greening scenarios in terms of outdoor thermal comfort or stress experienced during the heat wave via the UTCI, we first computed the UTCI for every hour of the six days of the 2003 heat wave (see Section 2.3). The UTCI values obtained were then sorted in the five heat stress classes described earlier (Table 3) to finally compute the mean time spent daily in each heat stress class (over the 6:00 to 22:00 time slot) for a person outside in the sun or in the shade.

Considering looking for shelter in the shade a fairly natural reflex in heat wave conditions, we focused the analysis of our greening scenarios on the daily impacts that they would have on the time spent at least in very strong heat stress (referred to as VSHS and corresponding to UTCI$>$ 38°C) by a person in the shade, across the entire simulation domain and across the three main types of urban fabric. These results are presented in Table 4.

As expected from previous impacts on street level temperatures, non-watered green roofs (GR) do not improve outdoor thermal comfort. Nevertheless, without modifying the total time spent in thermal heat stress, their watering (IGR) allows for the time spent at least in VSHS to be marginally decreased (by 15 min on average across the whole city). Note that watered green roofs appear more effective to improve street level thermal comfort in the dense collective housing fabric than in any other urban fabrics (22 min less spent at least in VSHS compared to 11 and 9 min less respectively in the Haussmannian and individual housing fabrics). This is explained by the high roof greening rate (Fig. 1) and the rather small street aspect ratios in this urban fabric (see Appendix A).

On the contrary, increasing ground vegetation in the city improves outdoor thermal comfort, by both increasing the time spent in thermal comfort and by reducing that spent in the various heat stress levels, with the most marked effect on VSHS. And

Table 4
Mean time (in hours and minutes) spent daily during the 2003 heatwave at least in very strong heat stress (UTCI $>$ 38 °C) for a person in the shade before greening (REF) and time reduction simulated for each greening scenarios. Means are calculated over daytime hours (06:00–22:00 LST), integrated across the entire urban zone and across the three main housing types and weighted by population density (estimated from national and public databases by Bonhomme, 2013).

Scenario	Town	Haussmannian buildings	Dense collective housing	Individual housing
Mean time spent at least in very strong heat stress				
REF	5:37	5:15	6:34	4:55
Impact of scenario				
GR	–	−0 : 01	+0 : 02	–
IGR	−0:15	−0:11	−0:22	−0:09
LV25	−0:20	−0:18	−0:26	−0:15
LV50	−0:39	−0:39	−0:49	−0:30
LV75	−0:55	−0:43	−1:10	−0:45
LHV25	−0:15	−0:21	−0:19	−0:10
LHV50	−0:37	−0:37	−0:49	−0:28
LHV75	−0:56	−0:51	−1:12	−0:43
LHV75-IGR	−1:04	−0:53	−1:24	−0:50

as expected, the greater the greening rate, the lower the time spent at least in VSHS. For low vegetation strategies for example (LV25, 50 and 75), the reduction in time spent at least in VSHS compared to the REF scenario (Table 4) goes from 20, to 39 and 55 min respectively on average across the whole city. In this case again, these scenarios are the most effective in the dense collective housing urban fabric. This is mainly explained by a greater increase in vegetation in this urban fabric compared to the Individual's and Haussmannian's (noticeable when comparing urban vegetation densities in Fig. 1 for each urban fabric).

Be it on average across the whole domain or across each urban fabric, the impact of wooded green spaces on VSHS seems to be of the same order of magnitude than that of green spaces with only low vegetation. Depending on the greening rate of each scenario family (LV versus LHV) and the urban fabric, the results of Table 4 showing impacts on VHS alone, do not allow for a systematic trend on the scenario family performance to be established. In order to draw a conclusion on the relative performances of low vegetation versus mixed wooded vegetation strategies in terms of thermal comfort, we need to account for the times spent in all the comfort and heat stress levels. Our average results across the whole domain show that the time a person in the shade would spend at least in VSHS (5:37 before greening) would decrease by 15 and 56 min for LHV25 and LHV75 against 20 and 55 min for LV25 and LV75 (Table 4), which is relatively similar. The combination of these figures shows that wooded green spaces (with 40% of deciduous trees) tend to be generally more effective to improve outdoor thermal comfort than those with only low vegetation, and this without even accounting for tree shading effects. Note also that our choice of triggering the watering at nighttime, which induces a weaker cooling during the day for wooded scenarios, does reduce in our simulations the potential of trees to improve outdoor thermal comfort during the day.

Finally, the scenario providing the best reduction in thermal heat stress is the combination of IGR and LHV75 with cumulative effects (LHV75-IGR in Table 4). Especially this combination allows for a person in the shade to spend daily 24 min more in thermal comfort as well as to spend 1 h less in VSHS. This combination presents the greatest potential in the dense collective housing fabric mainly because greater surfaces are available for greening.

3.2. Impacts on consumables: water for irrigation and energy for AC

In all scenarios, vegetation at ground level is systematically watered in summer, according to a predefined schedule. As the watering of green roofs is optional and the urban surfaces greened vary between scenarios, it is interesting to relate the benefits of the different greening strategies in terms of thermal comfort with their respective costs in water. These were calculated at the scale of the simulation domain (Fig. 6, right axis) before being compared to energy consumptions (Fig. 6, left axis).

3.2.1. Total water consumption

The variations in the water consumption simulated for irrigation are relatively important and are logically proportional to the increase in the urban vegetation surface of each scenario compared to the situation before greening (18.26 Mm^3): +11% for V25 scenarios (20.31 Mm^3), +22% for V50 scenarios (22.35 Mm^3), +34% for V75 scenarios (24.39 Mm^3), +29% for the IGR scenario (23.50 Mm^3), with the maximum of +62% obtained for the combined scenario LHV75-IGR (29.63 Mm^3). It is difficult to

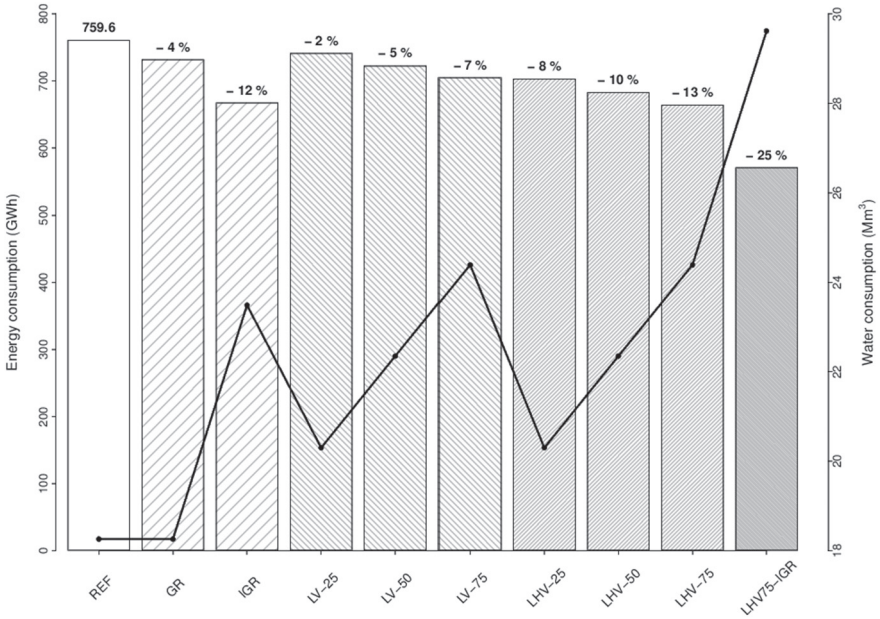

Fig. 6. Barplots (left axis) represent total energy consumptions during the 2003 heat wave without greening (REF) and with greening measures (with their respective percentage reductions). The black line (right axis) shows the total water consumptions devoted to the watering of urban green spaces (ground vegetation and green roofs when relevant) for all scenarios.

relate these values, which are very high, with known values of water consumption since very little is known on city-wide water consumptions for irrigation. For resource purposes, one may compare these consumptions to either the production of the non-potable water network of central Paris (coming from the river Seine and the Canal de l'Ourcq) which is about 200,000 m^3 day^{-1} (i.e. 1.2 Mm^3 for six days, Département du Val de Marne, 2016), or the low flow of the Seine (66 m^3 s^{-1}, Wikipedia, 2015) which might be experienced during summer dry spells, which is equivalent to 34.21 Mm^3 for six days. Compared to the production of non-potable water of central Paris, the consumptions of water associated with the various scenarios are disproportionate, but they nevertheless concern a much larger domain. These consumptions are equivalent to 53% (before greening), 59% (V25 scenarios), 65% (V50 scenarios), 71% (V75 scenarios), 69% (IGR) and 87% (LHV75-IGR) of the low flow of the Seine.

3.2.2. Total energy consumption

Such high water consumptions, however, are conducive to the reduction of energy consumption, as shown by the barplots of Fig. 6. These barplots represent the respective energy consumptions generated by the use of air-conditioning (AC) during the six days of the heat wave and cumulated over the entire urban domain. Note that in the present simulation configuration, it is chosen to only activate AC in office buildings, which actually represents a small proportion of the city at the resolution of 1 km (see map of building use in Appendix A). In this case, AC systems are controlled by a schedule set on office times and working days.

Before greening measures, the actual energy consumption, over the entire urban domain amounts to about 759 GWh (Fig. 6). Percentage figures show that the implementation of green roofs (GR), even if not watered, allows for the AC consumption to be reduced by 4%, which is explained by their insulating effect. Their watering (IGR) generates a significant reduction in energy consumption (12%), demonstrating once again that green roofs are only good performers if they are irrigated. This reduction level, which is well above those generally reached with ground greening (2–13 %), is moreover comparable to that generated with the mixed wooded vegetation scenario with the greatest greening rate (LHV75, 13%). Once again the effect of greening rate is clearly visible on Fig. 6, with as expected, the higher the greening rate, the lower the AC demand, hence the greater the energy reduction, with reductions of 2, 5 and 7% for scenarios LV25, LV50 and LV75, respectively. Comparing AC consumptions between scenario families with trees (LHV) and without trees (LV) shows that with equal consumptions of water, greening with trees is able to further reduce AC consumption than greening with low vegetation only (and this without accounting for shading effects). And this to such a point that the LV75 and LHV25 scenarios offer comparable energy reductions, which is an interesting result in terms of urban planning. A cumulative effect is obtained for the maximum combination of vegetation (LHV75-IGR) with a AC reduction of 25% as the processes involved in this reduction have two different origins: mainly insulation for green roofs and the cooling of air temperatures for ground vegetation.

3.2.3. Peak of energy demand

Although the total energy consumed during the heat wave is a relevant indicator to appreciate the respective performances of the greening scenarios, from a decision make perspective, the prediction of the peak of energetic demand during an extreme event is an even more useful indicator because it is very challenging to provide a city with a lot of energy in very little time. In our case, the energetic demand due to AC varies during the heat wave due to varying meteorological conditions but also due to the occupancy calendar of the buildings (offices). Its evolution with time under all the greening scenarios follows the same pattern as that of the REF scenario before greening (Fig. 7), with the maximum power (13.14 GW for REF) observed on August 12, the hottest day of the heat wave. This peak of energy demand is comparable to that recorded in the region Ile-de-France during the last cold spell (16.5 GW in February 2012, RTE [Réseau de transport d'électricité], 2016) which is therefore easy to produce

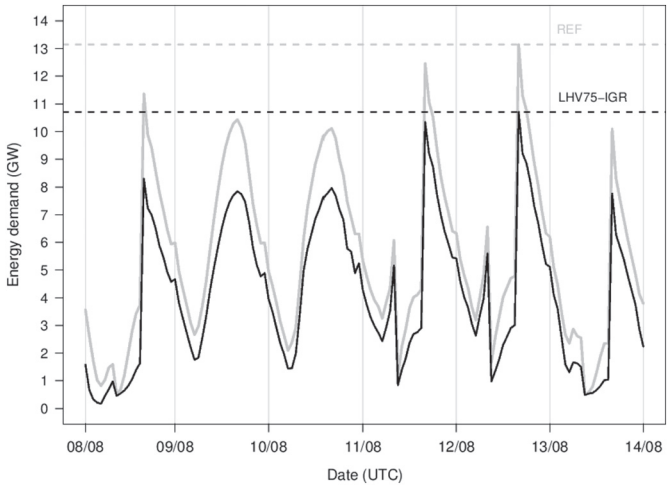

Fig. 7. Evolution of energy demand simulated during the 2003 heat wave without greening (REF) and with the most intense greening measure (LHV75-IGR), estimated from hourly instantaneous energy demands and spatially integrated over the urban areas of the whole domain.

by the current network of French nuclear reactors (about 58 reactors with a unit capacity of approximately 1 GW). However the AC demand simulated here is significantly underestimated since only office buildings are air-conditioned (and not residential buildings).

This peak of energy power during the 2003 heat wave is estimated for each greening scenario in order to measure their respective impacts at the height of the heat wave. Apart from the scenario with the maximum greening (LHV75-IGR) that achieves a reduction of the peak of energy power of about 18.5% (−2.43 GW, see Fig. 7), the most effective strategies are those with green roofs. And the comparison of the power peaks obtained for the scenarios with green roofs allows for us to quantify the relative energetic benefits of their insulation and evapotranspiration properties, with a reduction of the peak power of 1.17 GW for non-watered green roofs (related mainly to insulation) and a further reduction of 0.54 GW when they are watered (due to evapotranspiration). Next in descending order of performance are the mixed wooded vegetation scenarios with reductions ranging from 2.3 to 5.3% (0.3 to 0.7 GW) and those of low vegetation with reductions of between 1.4 and 4% (0.18 and 0.53 GW) depending on greening rate. As for the total energy consumption, the performance of the maximum vegetation combination (LHV75-IGR) in reducing the peak of energy power is due to cumulative impacts, which combine an action mainly on roof temperatures for irrigated green roofs and an action on street air temperatures for the ground vegetation.

4. Mean seasonal impacts

If one wants to enter the adaptation measures for cities within a framework of sustainable development, it is necessary to check that the impacts of these greening measures devised to meet the summer issues have no adverse effects on the rest of the year. With the simulation configuration setup for the present study (including a spatial resolution of 1 km and a simulation time step of 300 s), it is possible, due to the acceptable numerical cost, to simulate the previous greening scenarios for several years, in our case based on a 10-year meteorological forcing (1999–2008). Seasons cited thereafter are meteorological seasons. In this study we analyze the impact of the previous greening measures on the energy consumption related to the use of air conditioning and heating. We also address the issue of water management through the comparison of the amounts of surface water run off and those consumed for summer watering.

4.1. Impacts on heating and air-conditioning mean consumptions

During the simulation of the decade studied (1999–2008), and before greening (REF), the mean annual energy consumption at the scale of the simulation domain amounts to 86, 448 GWh with a standard deviation for the period of ±11, 507 GWh. The heating consumption is predominant in the present study, with 99.4% due to heating against only 0.6% due to AC. This reflects the choice to only activate the AC in offices (while the heating is activated in almost all buildings) and to assume a virtuous use of AC since the set-point temperature is prescribed to 26°C.

The greening strategy that generates the greatest impact on this annual energy consumption is undoubtedly the implementation of green roofs, whether they are watered or not (on average −5148 GWh which corresponds to a relative decrease of −6%). This result demonstrates the importance of insulation in terms of building energetics throughout the year (and the relevance of green roofs in this domain). Strategies with an increase in ground vegetation surfaces, have limited effects on building energetics because they act indirectly on the energy consumption by modifying outdoor microclimatic conditions locally, especially temperature and humidity. These effects vary with the type of vegetation: low vegetation causes a reduction in energy consumption, which is still very marginal (in the range of −0.1 to −0.3%) while the mixed wooded vegetation generates an overconsumption of energy (of around + 1.3%), mainly due to the overuse of heating. This overuse is a response to the lower street air temperatures caused by the mixed wooded vegetation all year round, even when the vegetation is not photosynthetically active (and which comes from the evaporation of the rainwater intercepted in this case).

For REF, the seasonal distribution of the annual energy consumption at the scale of the simulation domain is as followed: 60% in winter, 19% in spring, 1% in summer, and 20% in autumn. The part related to use of AC is only significant for summer season, during which it covers 60% of the energy consumption. The analysis of the seasonal effects of the different scenarios is presented hereafter through the difference in energy consumption that they generate compared to the situation before greening (Fig. 8).

A separate analysis of heating and AC consumptions highlights different behaviors between green roof and ground vegetation scenarios, which are consistent for all seasons. Note that both heating and AC are active all-year round and may be triggered during any season depending on internal building temperatures. To start with, the implementation of green roofs, thanks to their insulating properties, reduces both the demand for AC and heating, whatever the season. In summer, due to the additional evaporative cooling, this reduction amounts respectively for GR and IGR to −14% (GR) and −24% (IGR) for the demand for AC, and −45% and −38% for the heating demand (which is due to cold nights during the decade studied). Outside summer, they reduce the heating demand of −7.6% in autumn, of −4.5% in winter and of −8% in spring. Note that the better performances of the GR and IGR scenarios with regard to AC demand in summer (compared to those obtained during the heat wave of 2003, respectively −4 and −12%, Fig. 6) are explained by a greater availability of rainwater in summer (177 mm on average) than during the heat wave event of 2003 simulated, which favors a much larger evaporative cooling and results in a reduced use of AC. Wooded strategies that cool outside temperatures by evaporative cooling and solar radiation interception (effect not accounted for), have only beneficial effects on the energy consumption for AC, hence only in summer: this is illustrated by

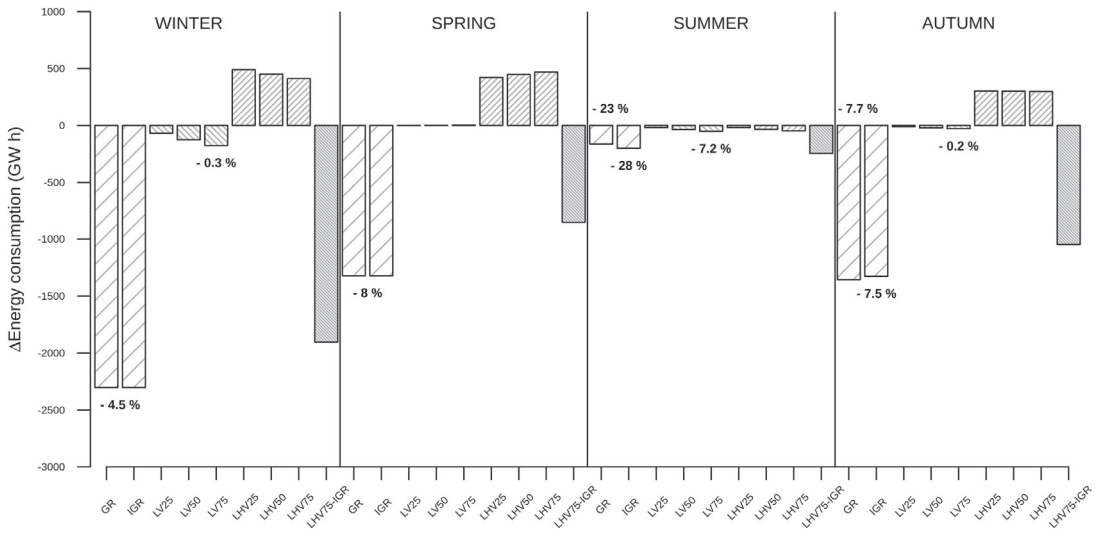

Fig. 8. Differences of seasonal energy consumptions (related to heating and air-conditioning) between each greening measures and without greening (REF), estimated from means over the 10-year period 1999–2008.

a reduction in the demand for AC of −15 to −23% to LHV25 and LHV75, i.e. for LHV25 a performance equivalent to that of GR and for LHV75 one equivalent to that of IGR. In parallel, these strategies do trigger more the use of heating resulting in an over-consumption of about 28% in summer, 2% in autumn, 1% in winter and 3% in spring, the highest being in summer because it's when the vegetation is the most active to cool the streets, hence nights are even cooler. The strategies based on low vegetation have the advantage of reducing AC consumption in summer from 5 to 13% but they also generate an overconsumption of summer heating of 2 to 6%. Outside summer, these strategies have little effect on the consumption of heating, since the reduction is less than 1% (LV75) in winter. Finally, the combination of green roofs and wooded vegetation provides beneficial effects at the scale of the city, both in terms of AC (−42 % in summer) and heating (−16% in summer, −6% in autumn, −4% in winter and −5% in spring) demands.

4.2. Impacts on urban surface run-off versus water consumption for irrigation

The greening of the city inevitably has an impact on the water balance of the city. And the knowledge of the respective volumes of water losses through runoff and water resources for irrigation is essential in the annual planning of water management at the scale of the city. So we quantified the impact of the different greening strategies on the surface runoff as well as those on the water consumed for summer watering. The runoff simulated by the model comes from three types of surface: the roofs of buildings, the roads and pavements, and the urban green spaces. On sealed surfaces such as roofs and roads, the runoff corresponds to the amount of rainwater intercepted that is not evaporated and exceeds the maximum interception capacity of roofs and roads (Lemonsu et al., 2007; Masson, 2000). For urban green spaces, it comes from a more complex water balance which is driven by the soil capacity to infiltrate water. With green roofs, a storage capacity may slightly change the balance compared to a natural soil (de Munck et al., 2013a).

Our simulation results show that there is no runoff from urban green areas, which means that the quantity of water intercepted by these surfaces are completely evaporated or infiltrated into the soil. Therefore, the surface runoff discussed thereafter comes exclusively from the street and roof contributions. Over the decade studied, for an average rainfall of 703 mm per year, the annual runoff integrated at city scale before greening amounts to 426 ± 124 Mm^3 (REF). A large inter-annual variability is noted in the decade studied, with values of standard deviations corresponding to 30–40% of average values. From a seasonal perspective, it is uniformly distributed over the year, with 103 ± 26 Mm^3 in winter, 96 ± 29 Mm^3 in spring (minimum), 112 ± 36 Mm^3 in summer and 115 ± 33 Mm^3 in autumn (maximum), for a distribution of seasonal rainfall of respectively 169, 169, 177 and 188 mm.

The various greening strategies significantly reduce annual runoff, with a greater efficiency of ground vegetation strategies over green roofs (from scenarios with a 50% greening rate). This result seems logical in the views of the respective volumes of soil available for water infiltration. With green roofs, the excess water is drained out of the roof, which participate to runoff. For ground vegetation scenarios, runoff reductions ranges from −11, −22 to −33% for greening rates of 25, 50 and 75% respectively, which logically corresponds to the rate of increase in urban vegetation generated by these scenarios. The maximum combination of vegetation (LHV75-IGR) generates the maximum runoff reduction (−35%).

The seasonal analysis of impacts on runoff (Fig. 9) shows a very positive effect of green roofs in spring (−18%) and in summer when they are not watered (−26%, GR). However, green roofs generate a slight increase in runoff in two cases. The first case is in winter (+4%, GR and IGR) when their soils are close to saturation and water loss through evapotranspiration is very limited. The

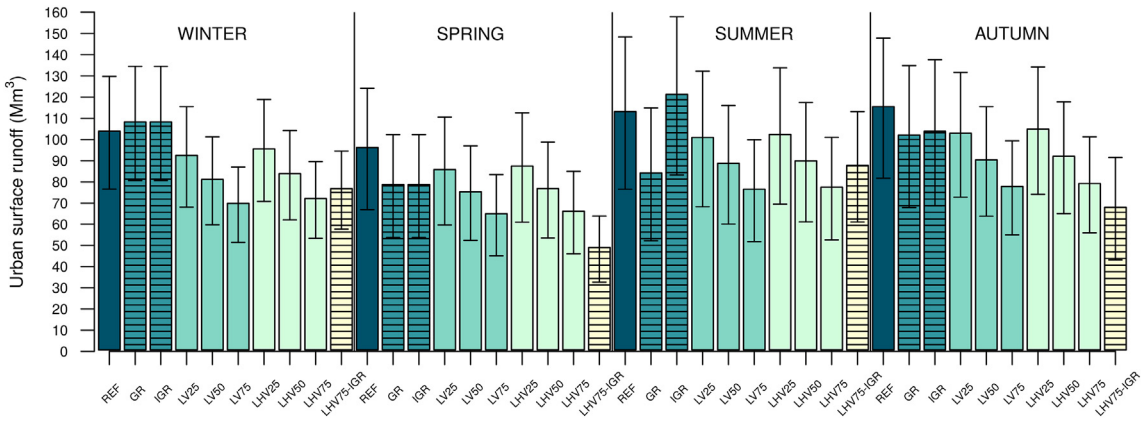

Fig. 9. Mean seasonal amounts of urban surface runoff (and standard deviations) before and after greening measures, estimated over the 10-year period 1999–2008 by spatial integration over the entire domain of road, roof and urban green space runoffs.

second case is in summer when they are irrigated (7%, IGR), suggesting that the volume chosen for irrigation to prevent hydric stress during the heat wave of 2003 is probably overrated for an average summer. Note however that as the parameterization used for the simulation of green roofs (de Munck et al., 2013a) tends to overestimate the drainage at the base of green roofs (hence their runoff), the retention capacity of such vegetated infrastructures may not be well enough captured in the current simulations. For ground vegetation strategies, seasonal performances are logically in line with their annual performance since they are proportional to the rate of increase in natural urban surfaces (−11, −22, and −33%).

As far as summer watering is concerned, since it is based on an automatic scheduler (fixed frequency and volume, identified for heat wave conditions), it is the same for each year of the decade studied: 282 Mm^3 city-wide and before greening. The watering of all urban green spaces under greening scenarios requests volumes of 362 Mm^3 for IGR, and from 314 to 346 and 378 Mm^3 for the ground vegetation scenarios respectively to greening rates 25, 50 and 75%. The maximum combination of vegetation (LHV75-IGR) logically needs the greatest volume for watering ground and roof vegetation (458 Mm^3).

5. Conclusions

A set of greening scenarios were simulated for the city of Paris to quantify the impacts of urban greening as an adaptation strategy to climate change in extreme summer conditions in order to improve outdoor thermal comfort and energy consumption for the cooling of buildings. Scenarios consisted in greening either 25, 50 or 75% of the urban ground available with low vegetation or with a mix of low vegetation and deciduous trees, or greening the roofs of compatible buildings, or both combined. These adaptation strategies were associated to a virtuous use of air-conditioning, and this only in office buildings. The simulation of the different scenarios was carried out by using a platform of models. In this configuration, the urban microclimate, as well as the levels of thermal comfort and energy consumption, which are good indicators of the city's vulnerability to heat wave, were estimated by a very detailed version of the Town Energy Balance model.

Our simulations in heat wave conditions showed that green roofs do not have an impact on 2-m street temperatures unless they are irrigated and that the cooling they induce remains limited (−0.25 to −0.5°C). Increasing ground vegetation is more efficient to cool the streets, with the higher the greening rate and the more the trees, the greater the cooling at night. Since the version of TEB used did not account for tree shading effects nor tree canopy radiative trapping, the differences in the amplitude of the cooling forecasted between the scenarios with low vegetation and those with a mixed wooded vegetation is essentially due to the higher foliar density of trees which induces a greater evapotranspiration, hence a greater cooling of the surrounding air. The cooling estimated in heat wave conditions varies between −0.5 and −2°C depending on the strategies. The maximum combination of greening measures (33% increase in urban vegetation over the entire geographic domain and a massive installation of irrigated green roofs on the buildings of Dense collective and Individual housings) allowed for a cooling of up to −3°C to be reached locally. For mixed wooded strategies, the cooling effect was more pronounced at night than daytime as a direct consequence of the timing chosen for irrigation (nighttime) and the method (sprinklers, simulated as artificial rainfall in the model). The cooling of street temperatures systematically lead to improving thermal comfort, with a significant reduction in the time spent in the different thermal stress levels, with up to one hour less spent in very high heat stress in the shade for the maximum combination of greening measures. However, the benefits obtained from mixed wooded scenarios may be underestimated since the model does not yet reproduce tree shading effects. Contrary to their low impact on outdoor thermal comfort, irrigated green roofs are effective to lower the energy consumption required for cooling the buildings in the course of a heat wave. This performance is explained by both their insulating properties and their evapotranspiration potential. Irrigated green roofs such as those developed in our scenario, allowed not only for the total energy consumption for AC to be reduced by 12% but also for the peak energy demand at the height of the heat wave to be lowered by 13%. Such a reduction in total energy consumption was only reached for the ground greening strategies with trees and the maximum greening rate (−13%) since ground vegetation

acts indirectly on the energy consumption of buildings. In line with the respective cooling of air temperatures induced, our simulations demonstrated that a small increase in urban green areas with trees had the same impact than a high increase in urban green areas with low vegetation only.

These performances both on improving the outdoor thermal comfort and the energy consumption of buildings for AC, however, have considerable water costs to be compared to the water supply that the city can receive during the other seasons as precipitation. Assuming that the surface runoff generated during the year on all urban surfaces could be stored to ensure summer watering of urban vegetation, the average annual runoff, estimated from ten years of simulation would ensure complete irrigation of urban vegetation only for the scenario with green roofs and the scenarios with the minimum increase in ground vegetation, suggesting that water resources should be found elsewhere if one was to increase urban vegetation coverage. The average summer impacts of greening strategies, estimated over ten years, show similar trends to those observed in a heat wave context, but of lesser magnitude. Throughout the year however, the increase in urban ground vegetation tends to lower outdoor temperatures (more marked with trees), resulting in a slight overconsumption of energy over the year due to an increase in heating demand (about 1%). Meanwhile, the insulating properties of green roofs allows for an annual energy savings of about 7% to be made, demonstrating the superior performance of green roofs on ground vegetation in terms of energy consumption reduction all year round. However, the slight overconsumption generated in present climate by the increase in ground vegetation with trees may not happen in future climate. Indeed in present climate, the annual energy consumption is mainly related to heating (a ratio of energy consumption for heating and AC of about 10 is estimated by Plazzotta (2015) for the same geographical domain and target temperatures hypotheses) when it is expected to be less than two by the end of the century, due to global warming.

The numerical modelling approach proposed in the present study, and especially the use of the TEB urban canopy model, are quite interesting and relevant tools in order to study and quantify greening scenarios at city scale. The results obtained however raise some questioning and highlight that additional developments and improvements are still required. Two main advances are currently in progress for TEB. A better representation of urban hydrological processes will be available soon, which includes an explicit description of water exchanges in urban underground, and of water transfers toward water supply and sewerage systems (Chancibault et al., 2015). In addition, a new parameterization has been implemented in order to simulate the radiation exchanges in urban canyons by accounting for tree canopy (Redon et al., in press). Accordingly, the energetic and aerodynamical exchanges will be also improved.

Also, as this study has shown, the choices made in the vegetation scenarios have consequences for the intensity and temporality of the impacts obtained. In order to help decision-making in a world where financial resources will be as limited as water and energy resources, it will be essential to assess, at the scale of a city studied, where greening strategies will be the most relevant to implement, while optimizing the use of water and the behavior of users in terms of energy. Water being a critical factor for the thermal performance of vegetation strategies, and climate projections being still uncertain regarding the future rain totals or frequencies, future studies should focus on scenarios combining urban greening and sustainable water management practices (water sensitive urban design) such as those proposed by Coutts et al. (2013), including green roofs with retention layers (that could be included in the existing greenroof module (de Munck et al., 2013a)). In the same spirit, it would be interesting to evaluate smart irrigation scenarios, e.g. with volumes of irrigation driven by soil moisture and/or air cooling needs).

At the same time, the question of the horizontal resolution at which these scenarios should be simulated arises. Indeed, the spatial resolution fixed in our study (1 km) was imposed by our will to evaluate at reasonable numerical cost, the impact of greening measures for a large geographical area, both at the scale of a heat wave event and on a seasonal basis over several years. However, urban planners and local authorities in charge of adaptation measures are working at a finer resolution for their implementation. Hence, we, modellers, need to simulate the physical processes involved in adaptation measures at smaller horizontal resolution (100 m or below) while at the same time providing impacts at the scale of the city and neighbourhoods. Therefore, the assessment of urban areas to be greened and their simulation should be carried out in the future at a horizontal resolution finer than the km.

Acknowledgments

This work has received support from the French Research National Agency (ANR) through two research projects: MUSCADE (Modélisation Urbaine et Stratégie d'adaptation au Changement climatique pour Anticiper la Demande et la production Énergétique, ANR-09-VILL-0003) and VegDUD (Rôle du végétal dans le Développement Urbain Durable, ANR-09-VILL-0007).

Appendix A. MUSCADE configuration

The MUSCADE configuration was established by all the partners of the MUSCADE project (Modélisation Urbaine et Stratégie d'adaptation au Changement climatique pour Anticiper la Demande et la production Énergétique) in order to carry out a prospective study, from today until 2100, of the interactions between city structure, construction processes, energy consumption, decentralized energy production, urban microclimate and climate change. The methodology underlying this configuration is detailed in Masson et al. (2014a) and summarized thereafter.

Table A1
Description of some building equipments, which are identical for all building types.

Equipment	Parameter	Value (building use)
Internal heat gains	Heat flux	5 W m^{-2} (Residential) 14 W m^{-2} (Office, Commercial, Industrial)
	Fraction of latent heat	20% (Residential) 10% (Office, Commercial, Industrial)
Heating	Temperature set point	19°C
Air-conditioning	Temperature set point	26°C
	Coefficient of performance (COP)	2.5
Solar protection	Active	Sun blinds (Office) Shutters (Residential)
	Solar factor	0.120 m (Office) 0.025 m (Residential)
Ventilation	Type	Controlled mechanical ventilation (CMV)
	Air exchange rate	0.7 vol h^{-1}
Extra-ventilation	Active	Residential
	System	Natural and mechanical
	Air exchange rate	Calculated by TEB

In order to simulate the evolution of the city and the energy-related processes in the MUSCADE project, a model platform was developed from several models. The Non-Equilibrium Model Urban-Dynamical Model (NEDUM, Viguié and Hallegatte, 2012; Viguié et al., 2014) was chosen to reproduce the socio-economic mechanisms underlying the urban system and thus is capable of simulating the socio-economic development of Paris from the 1900 until the end of the 21st century. Coupled with a geographical model (SLEUTH* Doukari et al., 2016), it allows for the spatial expansion of the city to be modelled. The description of urban morphology at the block scale is achieved through a new architectural model, the GENerator of Interactive Urban blockS (GENIUS, Bonhomme, 2013; Bonhomme et al., 2013), which can generate maps of urban blocks from public databases and architectural rules and simulate the evolution of these maps in time. Finally, the Town Energy Balance (TEB) urban canopy model (Masson, 2000) simulates the urban microclimate from the physical processes associated with urban geometry. The introduction into TEB of the Building Energy Model (BEM, Bueno et al., 2012; Pigeon et al., 2014) allows one to compute the energy balance of buildings and therefore to simulate the energy consumption at the scale of the city.

The spatial domain chosen for this configuration is a geographical area of 100 by 100 km around the city of Paris. From several national databases (for more details report to Bonhomme, 2013) and the outputs of the NEDUM-SLEUTH* model, GENIUS generates a map depicting the land use of the domain studied based on eight types of urban blocks (Continuous pavilion, Discontinuous pavilion, Continuous block, Discontinuous block, High-rise tower, Ancient centre, Industrial building). Based on their specific geometric features, these eight types of urban blocks are then translated into building types for TEB (Haussmannian, Individual housing, Dense collective housing, Office tower, Warehouse). Five types of building use (Residential, Office, Industrial, Agricultural, Commercial) complete this representation to modulate the use of equipments such as heating, air conditioning, or ventilation (Table A1) according to specific occupancy calendars (depending on the days of the week and hours of the day). Consistency between the different typologies is synthesized in Marchadier (2013). It is ultimately based on the types of buildings and their building dates (output by GENIUS) that are established the nature of the materials that make up the buildings (roofs, walls, windows, floor) and the associated thermal and radiative characteristics (Tables A2, A3, A4, A5 and A6) that are prescribed in each mesh of the domain studied to run TEB. Urban areas are then processed in a version of TEB that integrates recently developed functionalities, which allow one to evaluate many prospective scenarios while

Table A2
Description of radiative and thermal characteristics of Haussmannian buildings.

Haussmannian	<1900	1901–1917	1918–1944	1945–1974	1975–1999	2000–2011
Roof properties						
Layer 1 (external)						
Albedo (–)	0.6	0.6	0.6	0.6	0.6	0.6
Emissivity (–)	0.3	0.3	0.3	0.3	0.3	0.3
Heat capacity (kJ m^{-3} K^{-1})	2736	2736	2736	2736	2736	2736
Thermal conductivity (W m^{-1} K^{-1})	110	110	110	110	110	110
Width (m)	0.0008	0.0008	0.0008	0.0008	0.0009	0.0008
Layer 2						
Heat capacity (kJ m^{-3} K^{-1})	900	900	900	900	900	900
Thermal conductivity (W m^{-1} K^{-1})	0.13	0.13	0.13	0.13	0.13	0.13
Width (m)	0.02	0.02	0.02	0.02	0.02	0.02
Layer 3 (internal)						
Heat capacity (kJ m^{-3} K^{-1})	800	800	800	800	800	800
Thermal conductivity (W m^{-1} K^{-1})	0.13	0.13	0.13	0.13	0.13	0.13
Width	0.02	0.02	0.02	0.02	0.02	0.02

(*continued on next page*)

Table A2 (*continued*)

Haussmannian	<1900	1901–1917	1918–1944	1945–1974	1975–1999	2000–2011
Facade (wall and glazing) properties						
Layer 1 (external)						
Albedo (–)	0.4	0.4	0.4	0.4	0.4	0.4
Emissivity (–)	0.9	0.9	0.9	0.9	0.9	0.9
Heat capacity (kJ m^{-3} K^{-1})	2000	2000	2000	2000	2000	2000
Thermal conductivity (W m^{-1} K^{-1})	1.4	1.4	1.4	1.4	1.4	1.4
Width (m)	0.1	0.1	0.1	0.1	0.1	0.1
Layer 2						
Heat capacity (kJ m^{-3} K^{-1})	2000	2000	2000	2000	2000	2000
Thermal conductivity (W m^{-1} K^{-1})	1.4	1.4	1.4	1.4	1.4	1.4
Width (m)	0.1	0.1	0.1	0.1	0.1	0.1
Layer 3						
Heat capacity (kJ m^{-3} K^{-1})	2000	2000	2000	2000	2000	2000
Thermal conductivity (W m^{-1} K^{-1})	1.4	1.4	1.4	1.4	1.4	1.4
Width (m)	0.1	0.1	0.1	0.1	0.1	0.1
Layer 4 (internal)						
Heat capacity (kJ m^{-3} K^{-1})	700	700	700	700	700	700
Thermal conductivity (W m^{-1} K^{-1})•2	0.2	0.2	0.2	0.2	0.2	0.2
Width (m)	0.03	0.03	0.03	0.03	0.03	0.03
Glazing						
Solar factor (–)	0.6	0.6	0.6	0.6	0.5	0.5
U-factor (W m^{-2} K^{-1})	6.0	6.0	6.0	6.0	3.5	2.3
Facade fraction (%)	0.25	0.25	0.25	0.25	0.25	0.25
Floor properties						
Layer 1 (bottom)						
Heat capacity (kJ m^{-3} K^{-1})	800	800	800	800	800	800
Thermal conductivity (W m^{-1} K^{-1})	0.3	0.3	0.3	0.3	0.3	0.3
Width (m)	0.1	0.1	0.1	0.1	0.1	0.1
Layer 2						
Heat capacity (kJ m^{-3} K^{-1})	800	800	800	800	800	800
Thermal conductivity (W m^{-1} K^{-1})	0.3	0.3	0.3	0.3	0.3	0.3
Width	0.1	0.1	0.1	0.1	0.1	0.1
Layer 3 (top)						
Heat capacity (kJ m^{-3} K^{-1})	900	900	900	900	900	900
Thermal conductivity (W m^{-1} K^{-1})	0.13	0.13	0.13	0.13	0.13	0.13
Width (m)	0.02	0.02	0.02	0.02	0.02	0.02

maintaining a decent computational cost: a Surface Boundary Layer model that solves vertical turbulent diffusion within multilayer street canyons (Hamdi and Masson, 2008; Masson and Seity, 2009), a new urban weather generator (UWG Le Bras and Masson, 2015) that derives a 2D temperature forcing (urban heat island at forcing level) from 1D atmospheric forcings and city characteristics, the BEM model for evaluating energy demand (Bueno et al., 2012; Pigeon et al., 2014), the Veg (Lemonsu et al., 2012) and GREENROOF (de Munck et al., 2013a) modules to better simulate building-vegetation interactions, as well a module for computing thermal comfort indexes (Fiala et al., 2012; Pigeon, 2011). For computational cost considerations, initial input data provided by GENIUS at a 250 m resolution are aggregated at 1 km by TEB at the beginning of each simulation. The rules set up for this aggregation is to retain the dominant building type (and therefore its radiative and thermal characteristics) and to average the geometric characteristics of buildings.

Table A3
Description of radiative and thermal characteristics of Individual housings.

Individual housings	<1900	1901–1917	1918–1944	1945–1974	1975–1999	2000–2011
Roof properties						
Layer 1 (external)						
Albedo (–)	0.2	0.2	0.2	0.2	0.2	0.2
Emissivity (-)	0.8	0.8	0.8	0.8	0.8	0.8
Heat capacity (kJ m^{-3} K^{-1})	1600	1600	1600	1600	1600	1600
Thermal conductivity (W m^{-1} K^{-1})	1	1	1	1	1	1
Width (m)	0.025	0.025	0.025	0.025	0.025	0.025
Layer 2						
Heat capacity (kJ m^{-3} K^{-1})	75	75	75	75	75	75
Thermal conductivity (W m^{-1} K^{-1})	0.035	0.035	0.025	0.035	0.035	0.025
Width (m)	0.01	0.01	0.01	0.01	0.05	0.15
Layer 3 (internal)						
Heat capacity (kJ m^{-3} K^{-1})	800	800	800	800	800	800
Thermal conductivity (W m^{-1} K^{-1})	0.13	0.13	0.13	0.13	0.13	0.13
Width (m)	0.01	0.01	0.01	0.01	0.01	0.01

Table A3 (*continued*)

Individual housings	<1900	1901–1917	1918–1944	1945–1974	1975–1999	2000–2011
Facade (wall and glazing) properties						
Layer 1 (external)						
Albedo (–)	0.4	0.4	0.25	0.4	0.4	0.4
Emissivity (–)	0.9	0.9	0.9	0.9	0.9	0.9
Heat capacity (kJ m^{-3} K^{-1})	2000	1600	1600	1800	1800	1800
Thermal conductivity (W m^{-1} K^{-1})	1.4	0.8	0.8	1	1	1
Width (m)	0.05	0.05	0.03	0.04	0.03	0.03
Layer 2						
Heat capacity (kJ m^{-3} K^{-1})	2000	2200	1480	2200	2200	2200
Thermal conductivity (W m^{-1} K^{-1})	1.4	1.4	1.15	1.75	0.04	0.04
Width (m)	0.15	0.15	0.15	0.11	0.17	0.17
Layer 3						
Heat capacity (kJ m^{-3} K^{-1})	2000	2200	1480	2200	51	51
Thermal conductivity (W m^{-1} K^{-1})	1.4	1.4	1.15	1.75	0.04	0.04
Width (m)	0.15	0.15	0.13	0.04	0.04	0.08
Layer 4 (internal)						
Heat capacity (kJ m^{-3} K^{-1})	700	700	700	700	700	700
Thermal conductivity (W m^{-1} K^{-1})	0.2	0.2	0.2	0.2	0.2	0.2
Width (m) Albedo (–)	0.03	0.03	0.03	0.02	0.015	0.013
Glazing						
Solar factor (–)	0.6	0.6	0.6	0.6	0.5	0.5
U-factor (W m^{-2} K^{-1})	6.0	6.0	6.0	6.0	3.5	2.3
Facade fraction (%)	0.15	0.15	0.15	0.15	0.15	0.15
Floor properties						
Layer 1 (bottom)						
Heat capacity (kJ m^{-3} K^{-1})	2200	2200	2200	2200	2200	2200
Thermal conductivity (W m^{-1} K^{-1})	1.65	1.65	1.65	1.65	1.65	1.65
Width (m)	0.1	0.1	0.1	0.1	0.1	0.1
Layer 2						
Heat capacity (kJ m^{-3} K^{-1})	2200	2200	2200	2200	2200	2200
Thermal conductivity (W m^{-1} K^{-1})	1.65	1.65	1.65	1.65	1.65	1.65
Width (m)	0.1	0.1	0.1	0.1	0.1	0.1
Layer 3 (top)						
Heat capacity (kJ m^{-3} K^{-1})	2200	2200	2200	2200	2200	2200
Thermal conductivity (W m^{-1} $K^{/}$ – 1)	1.65	1.65	1.65	1.65	1.65	1.65
Width (m)	0.02	0.02	0.02	0.02	0.02	0.02

Table A4
Description of radiative and thermal characteristics of Dense collective housings.

Collective housings	<1900	1901–1917	1918–1944	1945–1974	1975–1999	2000–2011
Roof properties						
Layer 1(external)						
Albedo (–)	0.2	0.2	0.2	0.2	0.2	0.2
Emissivity (–)	0.8	0.8	0.8	0.8	0.8	0.8
Heat capacity (kJ m^{-3} K^{-1})	2100	2100	2100	2100	2100	2100
Thermal conductivity (W m^{-1} K^{-1})	0.7	0.7	0.7	0.7	0.7	0.7
Width (m)	0.004	0.004	0.004	0.004	0.004	0.004
Layer 2						
Heat capacity (kJ m^{-3} K^{-1})	75	75	75	75	75	75
Thermal conductivity (W m^{-1} K^{-1})	0.035	0.035	0.025	0.035	0.035	0.025
Width (m)	0.01	0.01	0.01	0.01	0.1	0.1
Layer 3 (internal)						
Heat capacity (kJ m^{-3} K^{-1})	2300	2300	2300	2300	2300	2300
Thermal conductivity (W m^{-1} K^{-1})	2.3	2.3	2.3	2.3	2.3	2.3
Width (m)	0.2	0.2	0.2	0.2	0.2	0.2
Facade (wall and glazing) properties						
Layer 1 (external)						
Albedo (–)	0.4	0.4	0.2	0.4	0.4	0.4
Emissivity (–)	0.9	0.9	0.9	0.9	0.9	0.9
Heat capacity (kJ m^{-3} K^{-1})	2000	1600	1600	1800	1800	1800
Thermal conductivity (W m^{-1} K^{-1})	1.4	0.8	0.8	1	1	1
Width (m)	0.02	0.02	0.03	0.04	0.03	0.03
Layer 2						
Heat capacity (kJ m^{-3} K^{-1})	2000	2200	1480	2200	2200	2200
Thermal conductivity (W m^{-1} K^{-1})	1.4	1.7	1.2	1.65	1.65	1.65
Width (m)	0.15	0.15	0.15	0.15	0.2	0.2

(*continued on next page*)

Table A4 (*continued*)

Collective housings	<1900	1901–1917	1918–1944	1945–1974	1975–1999	2000–2011
Layer 3						
Heat capacity (kJ m^{-3} K^{-1})	2000	2200	1480	2200	51	51
Thermal conductivity (W m^{-1} K^{-1})	1.4	1.4	1.15	1.75	0.04	0.04
Width (m)	0.15	0.15	0.13	0.1	0.04	0.08
Layer 4 (internal)						
Heat capacity (kJ m^{-3} K^{-1})	700	700	700	700	700	700
Thermal conductivity (W m^{-1} K^{-1})	0.2	0.2	0.2	0.2	0.2	0.2
Width (m)	0.03	0.03	0.03	0.02	0.015	0.013
Glazing						
Solar factor (–)	0.6	0.6	0.6	0.6	0.5	0.5
U-factor (W m^{-2} K^{-1})	6	6	6	6	3.5	2.3
Facade fraction (%)	0.4	0.4	0.4	0.4	0.4	0.4
Floor properties						
Layer 1 (bottom)						
Heat capacity (kJ m^{-3} K^{-1})	2200	2200	2200	2200	2200	2200
Thermal conductivity (W m^{-1} K^{-1})	1.65	1.65	1.65	1.65	1.65	1.65
Width (m)	0.1	0.1	0.1	0.1	0.1	0.1
Layer 2						
Heat capacity (kJ m^{-3} K^{-1})	2200	2200	2200	2200	2200	2200
Thermal conductivity (W m^{-1} K^{-1})	1.65	1.65	1.65	1.65	1.65	1.65
Width (m)	0.1	0.1	0.1	0.1	0.1	0.1
Layer 3 (top)						
Heat capacity (kJ m^{-3} K^{-1})	2200	2200	2200	2200	2200	2200
Thermal conductivity (W m^{-1} K^{-1})	1.65	1.65	1.65	1.65	1.65	1.65
Width (m)	0.02	0.02	0.02	0.02	0.02	0.02

The present study aimed at evaluating the impacts of greening scenarios is based on the map of Paris in present time (as opposed to future scenarios). Some of the main surface characteristics obtained through this MUSCADE configuration are presented Fig. A1. The map representing the fraction of existing urban vegetation in present time can be found on Fig. 1.

Table A5
Description of radiative and thermal characteristics of offices towers.

Office towers	<1900	1901–1917	1918–1944	1945–1974	1975–1999	2000–2011
Roof properties						
Layer 1 (external)						
Albedo (–)	0.2	0.2	0.2	0.2	0.2	0.2
Emissivity (–)	0.8	0.8	0.8	0.8	0.8	0.8
Heat capacity (kJ m^{-3} K^{-1})	2100	2100	2100	2100	2100	2100
Thermal conductivity (W m^{-1} K^{-1})	0.7	0.7	0.7	0.7	0.7	0.7
Width (m)	0.004	0.004	0.004	0.004	0.004	0.004
Layer 2						
Heat capacity (kJ m^{-3} K^{-1})	75	75	75	75	75	75
Thermal conductivity (W m^{-1} K^{-1})	0.035	0.035	0.035	0.035	0.035	0.035
Width (m)	0.01	0.01	0.01	0.01	0.1	0.1
Layer 3 (internal)						
Heat capacity (kJ m^{-3} K^{-1})	2300	2300	2300	2300	2300	2300
Thermal conductivity (W m^{-1} K^{-1})	2.3	2.3	2.3	2.3	2.3	2.3
Width (m)	0.2	0.2	0.2	0.2	0.2	0.2
Facade (wall and glazing) properties						
Layer 1 (external)						
Albedo (–)	0.4	0.4	0.25	0.4	0.4	0.4
Emissivity (–)	0.9	0.9	0.9	0.9	0.9	0.9
Heat capacity (kJ m^{-3} K^{-1})	2000	1600	1600	1800	1800	1800
Thermal conductivity (W m^{-1} K^{-1})	1.4	0.8	0.8	1	1	1
Width (m)	0.02	0.03	0.03	0.04	0.03	0.03
Layer 2						
Heat capacity (kJ m^{-3} K^{-1})	2000	2200	1480	2200	2200	2200
Thermal conductivity (W m^{-1} K^{-1})	1.4	1.7	1.2	1.65	1.65	1.65
Width (m)	0.1	0.15	0.15	0.15	0.2	0.2
Layer 3						
Heat capacity (kJ m^{-3} K^{-1})	2000	2200	1480	2200	51	51
Thermal conductivity (W m^{-1} K^{-1})	1.4	1.4	1.15	1.75	0.04	0.04
Width (m)	0.1	0.25	0.13	0.035	0.04	0.0.08
Layer 4 (internal)						
Heat capacity (kJ m^{-3} K^{-1})	700	700	700	700	700	700
Thermal conductivity (W m^{-1} K^{-1})	0.2	0.2	0.2	0.2	0.2	0.2
Width (m)	0.03	0.03	0.03	0.02	0.015	0.013

Table A5 (*continued*)

Office towers	<1900	1901–1917	1918–1944	1945–1974	1975–1999	2000–2011
Glazing						
Solar factor (–)	0.6	0.6	0.6	0.6	0.5	0.5
U-factor (W m^{-2} K^{-1})	6	6	6	3.5	2.3	
Facade fraction (%)	0.8	0.8	0.8	0.8	0.8	0.8
Floor properties						
Layer 1 (bottom)						
Heat capacity (kJ m^{-3} K^{-1})	2200	2200	2200	2200	2200	2200
Thermal conductivity (W m^{-1} K^{-1})	1.65	1.65	1.65	1.65	1.65	1.65
Width (m)	0.1	0.1	0.1	0.1	0.1	0.1
Layer 2						
Heat capacity (kJ m^{-3} K^{-1})	2200	2200	2200	2200	2200	2200
Thermal conductivity (W m^{-1} K^{-1})	1.65	1.65	1.65	1.65	1.65	1.65
Width (m)	0.1	0.1	0.1	0.1	0.1	0.1
Layer 3 (top)						
Heat capacity (kJ m^{-3} K^{-1})	2200	2200	2200	2200	2200	2200
Thermal conductivity (W m^{-1} K^{-1})	1.65	1.65	1.65	1.65	1.65	1.65
Width (m)	0.02	0.02	0.02	0.02	0.02	0.02

Table A6
Description of radiative and thermal characteristics of warehouses.

Warehouses	<1900	1901–1917	1918–1944	1945–1974	1975–1999	2000–2011
Roof properties						
Layer 1 (external)						
Albedo (–)	0.2	0.2	0.2	0.2	0.5	0.5
Emissivity (–)	0.8	0.8	0.8	0.8	0.3	0.3
Heat capacity (kJ m^{-3} K^{-1})	1600	1600	1600	1600	3500	3500
Thermal conductivity (W m^{-1} K^{-1})	1	1	1	1	50	50
Width (m)	0.03	0.03	0.03	0.03	0.001	0.001
Layer 2						
Layer 3 (internal)						
Heat capacity (kJ m^{-3} K^{-1})	900	900	900	900	3500	3500
Thermal conductivity (W m^{-1} K^{-1})	0.13	0.13	0.13	0.13	50	50
Width (m)	0.05	0.05	0.05	0.05	0.05	0.05
Facade (wall and glazing) properties						
Layer 1 (external)						
Albedo (–)	0.4	0.4	0.4	0.4	0.3	0.3
Emissivity (–)	0.9	0.9	0.9	0.9	0.5	0.5
Heat capacity (kJ m^{-3} K^{-1})	1800	1800	1800	1800	3500	3500
Thermal conductivity (W m^{-1} K^{-1})	1	1	1	1	50	50
Width (m)	0.03	0.03	0.03	0.00	0.001	0.001
Layer 2						
Heat capacity (kJ m^{-3} K^{-1})	1480	1480	1480	2200	75	75
Thermal conductivity (W m^{-1} K^{-1})	1.2	1.2	1.2	1.65	0.035	0.035
Width (m)	0.1	0.1	0.1	0.1	0.025	0.025
Layer 3						
Heat capacity (kJ m^{-3} K^{-1})	1480	1480	1480	2200	3500	3500
Thermal conductivity (W m^{-1} K^{-1})	1.2	1.2	1.2	1.65	50	50
Width (m)	0.1	0.1	0.1	0.1	0.03	0.0.03
Layer 4 (internal)						
Heat capacity (kJ m^{-3} K^{-1})	700	700	700	700	700	700
Thermal conductivity (W m^{-1} K^{-1})	0.2	0.2	0.2	0.2	0.2	0.2
Width (m)	0.03	0.03	0.03	0.03	0.03	0.03
Glazing						
Solar factor (–)	0.6	0.6	0.6	0.6	0.5	0.5
U-factor (W m^{-2} K^{-1})	6	6	6	3.5	2.3	
Facade fraction (%)	0	0	0	0	0	0
Floor properties						
Layer 1 (bottom)						
Heat capacity (kJ m^{-3} K^{-1})	2200	2200	2200	2200	3500	3500
Thermal conductivity (W m^{-1} K^{-1})	1.65	1.65	1.65	1.65	50	50
Width (m)	0.1	0.1	0.1	0.1	0.02	0.02
Layer 2						
Heat capacity (kJ m^{-3} K^{-1})	2200	2200	2200	2200	3500	3500
Thermal conductivity (W m^{-1} K^{-1})	1.65	1.65	1.65	1.65	50	50
Width (m)	0.1	0.1	0.1	0.1	0.02	0.02
Layer 3 (top)						
Heat capacity (kJ m^{-3} K^{-1})	2200	2200	2200	2200	400	400
Thermal conductivity (W m^{-1} K^{-1})	1.65	1.65	1.65	1.65	0.1	0.1
Width (m)	0.02	0.02	0.02	0.02	0.005	0.005

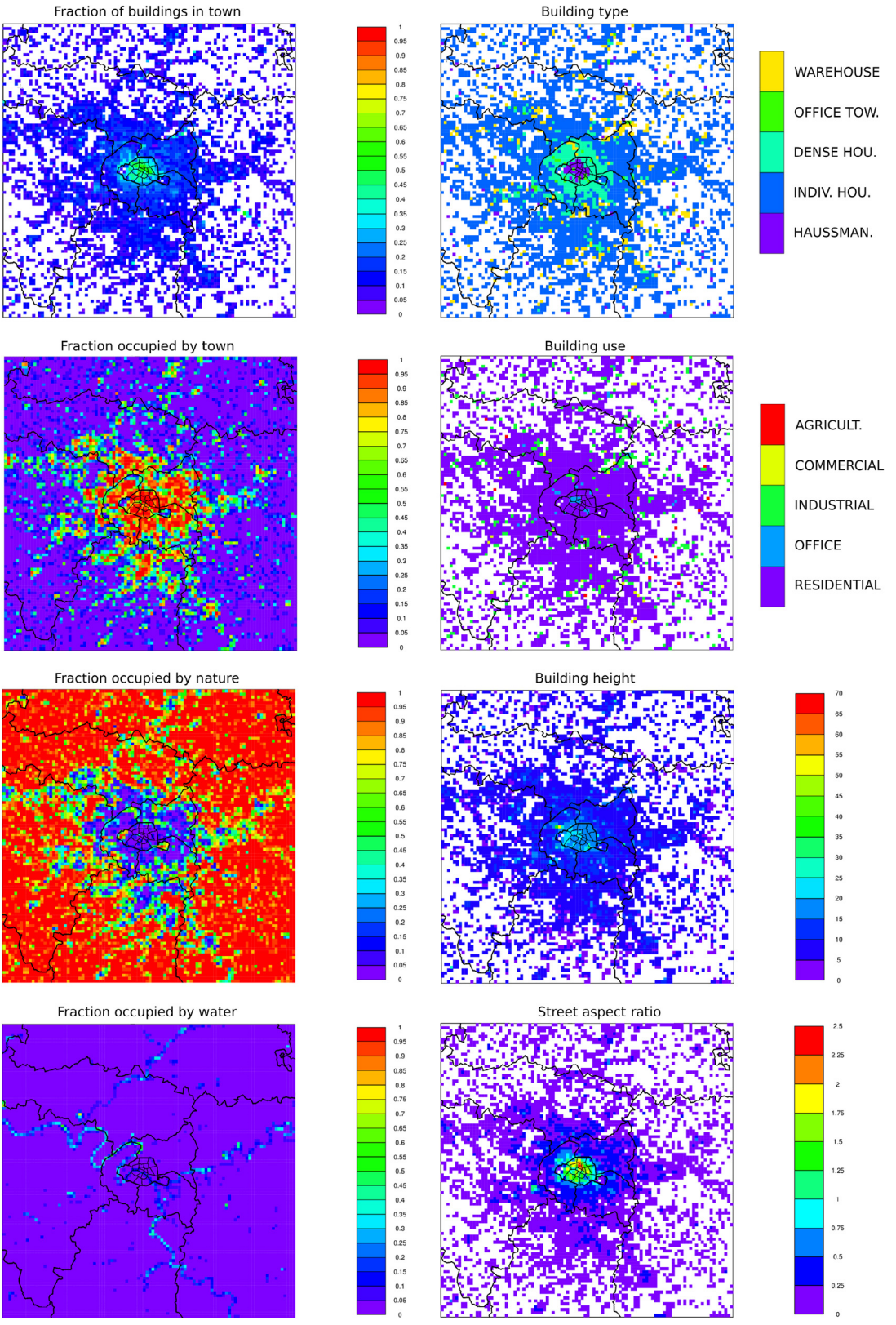

Fig. A1. Maps representing within each 1 km^2 mesh of the simulation domain the fractions of natural and artificial surfaces, the fraction of inland water, the fraction of buildings and the associated building types and usages, as well as their height and the street aspect ratio.

Appendix B. Comparison of observed and simulated temperature series for the REFERENCE simulation

For the evaluation of the reference simulation, we retained weather stations within the simulation domain that hold both hourly records of 2-m temperatures during the six-days of the 2003 heat wave and minimum and maximum daily records for the 1999–2008 decade studied. Fig. B1 shows where they are located in the simulation domain.

As part of the evaluation exercise of the REFERENCE simulation, the evolution of hourly 2-m air temperatures observed and simulated during the 2003 heat wave have been compared (Fig. B2). This illustrates how well the model estimates relate to the observations, and this for two sets of weather stations, *urban* and *rural* stations (Fig. B1). The model simulates well the daily dynamics of the air temperatures at 2-m, with variations of similar amplitudes (5.22 °C in the simulation versus 5.06 °C in the observations at urban stations and respectively 6.03 and 5.51 °C at rural stations). However temperatures are on average overestimated, be it at urban or rural stations, with a mean bias of respectively +1.33 °C and +1.14 °C and errors of 1.9 °C for both types of stations. These mean biases seem to be the consequence of an overestimation of the temperatures simulated in the first three days and the last days of the heat wave (08–10 and 13 August 2003), be it at urban or rural stations. One of the probable reasons for these inter-daily differences is the change in wind regime observed between the first two days of the simulation and the subsequent ones. Indeed, a different wind regime, mostly from the north, is observed on all the stations on the first two and the last day of the heat wave, probably causing slightly cooler temperatures than with a different wind regime. The differences between observed and simulated temperatures for these days coinciding with northern winds would therefore suggest that the models configuration that we used does not allow for the temperature variations by advection of the air masses to be fully well simulated.

The temperature anomaly between the two sets of weather stations (urban and rural) has also been calculated during the heat wave, in the same spirit as for the calculation of an urban heat island intensity. Its evolution during the six days of the heat wave is presented on the right hand side graph of Fig. B2. This observed anomaly varies between 0.15 °C ± 0.27 °C in the middle of the day and 2.34 °C ± 0.38 °C in the middle of the night. The temperature anomaly simulated by the model shows a good agreement with that observed (R=0.73), especially at daytime. As expected from previous results, this anomaly is overestimated by the model, with a mean biais of +0.19 °C and errors of 0.74 °C.

The mean annual cycles of the minimum and maximum daily temperature means have been plotted on Fig. B3 for the same two types of weather stations. As expected, the annual cycles of simulated and observed monthly means of 2-m temperatures are well correlated, be it for urban or rural stations, except for the TX mean in July. Fig. B3 illustrates well the model tendency to overestimate monthly means of minimum and maximum temperatures, with an equivalent biais at daytime and nighttime for rural stations (around 0.75 °C) and a more important biais at nighttime than daytime for urban stations (associated MBE values can be found in Table 1).

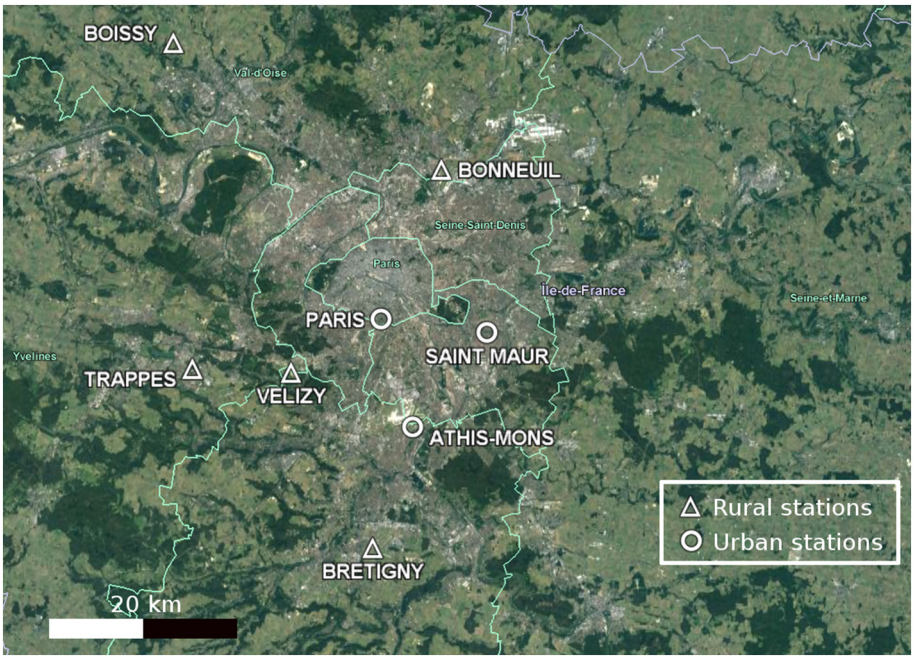

Fig. B1. Map showing the locations of the weather stations available for the evaluation exercise, as well as their type, urban or rural, depending on the surface characteristics of their nearest grid point at the resolution of 1-km.

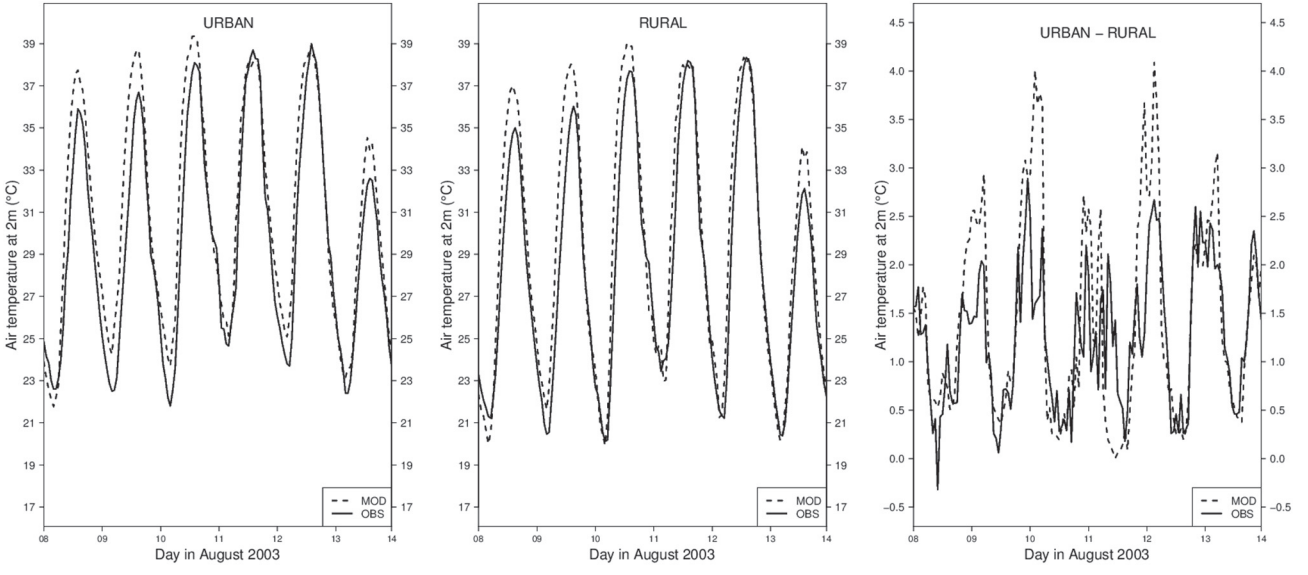

Fig. B2. Left and centre: 2-m air temperature evolution observed and simulated (REF scenario - before greening) during the six days of the 2003 heat wave for urban and rural weather stations. Right: 2-m air temperature anomaly between urban and rural weather stations during the six days of the 2003 heat wave.

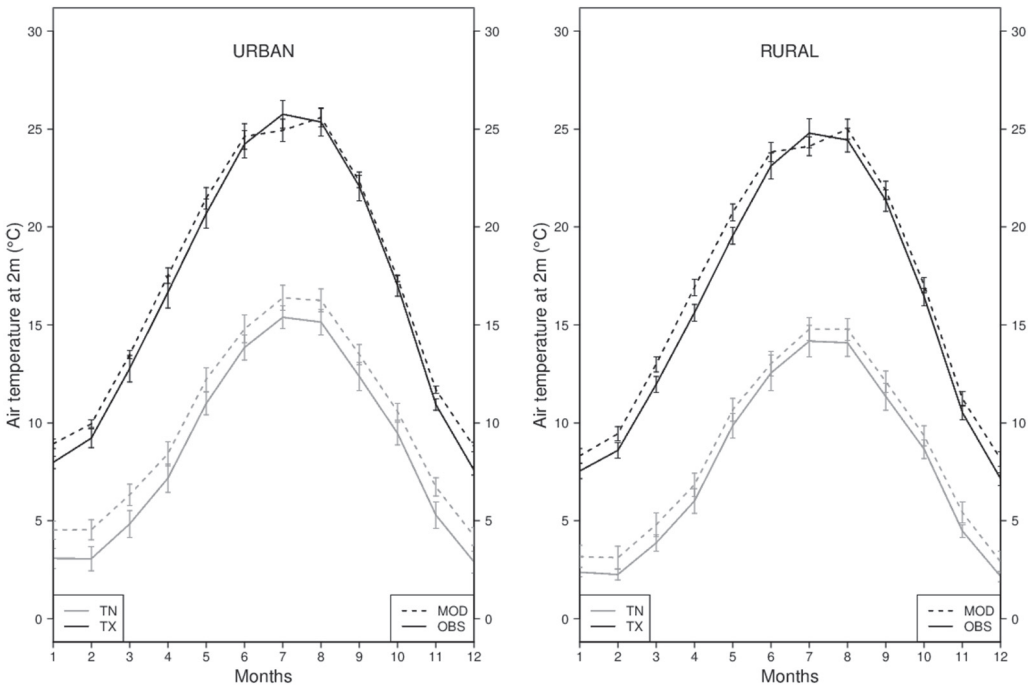

Fig. B3. Mean annual cycles of 2-m air temperatures (and associated standard deviations) observed and simulated (REF scenario - before greening) over the 10-year period 1999–2008 for urban and rural stations, computed from daily minimum and maximum daily temperatures (respectively named TN and TX).

References

Adnot, J., 2003a. Energy Efficiency and Certification of Central Air Conditioners. Study for the D.G. Transportation-Energy (DGTREN) of the Commission of the EU . Ed. ARMINES. Final report, vol 1, April 2003.

Adnot, J., 2003b. Energy Efficiency and Certification of Central Air Conditioners. Study for the D.G. Transportation-Energy (DGTREN) of the Commission of the EU . Ed. ARMINES. Final report, vol 3, April 2003.

Ashley, R., Nowell, R., Gersonius, B., Walker, L., 2011. A Review of Current Knowledge. Surface Water Management and Urban Green Infrastructure. A Review of Potential Benefits and UK and International Practices.

Barradas, V., 1991. Air temperature and humidity and human comfort index of some city parks of Mexico City. Int. J. Biometeorol. 35, 24–28.

Bass, B., Krayenhoff, E.S., Martilli, A., Stull, R.B., Auld, H., 2003. The impact of green roofs on torontos urban heat island. Proceedings of the First North American Green Roof Conference: Greening Rooftops for Sustainable Communities. pp. 292–304.

Bonhomme, M., 2013. Contribution à la génération de bases de données multi-scalaires et évolutives pour une approche pluridisciplinaire de lénergétique urbaine. INSA, Institut National des Sciences Appliquées de Toulouse, France. Ph.D. thesis.

Bonhomme, M., Masson, V., Adolphe, L., Faraut, S., 2013. Genius: A tool for multi-disciplinary and multi-scalar databases. AGU Fall Meeting Abstracts. pp. 1018.

Boone, A., 2000. Modélisation des processus hydrologiques dans le schéma de surface ISBA: Inclusion dun reservoir hydrologique, du gel et modelisation de la neige. Université Paul Sabatier, Toulouse, France. Ph.D. thesis.

Bowler, D.E., Buyung-Ali, L., Knight, T.M., Pullin, A.S., 2010. Urban greening to cool towns and cities: a systematic review of the empirical evidence. Landsc. Urban Plan. 97, 147–155.

Bueno, B., Pigeon, G., Norford, L., Zibouche, K., M., C, 2012. Development and evaluation of a building energy model integrated in the teb scheme. Geosci. Model Dev. 5, 433–448.

Castleton, H., Stovin, V., Beck, S., Davison, J., 2010. Green roofs; building energy savings and the potential for retrofit. Energ. Buildings 41, 1582–1591.

V, M., Chancibault, K., Brun, J.-M., Allard, A., Andrieu, H., Lemonsu, A., de Munck, C., 2015. Improving the water budget in the urban surface scheme teb for a better evaluation of greening strategies for adaptation purposes. ICUC 9, 9th International conference on Urban climate, 20-24 July, 2015, Toulouse, France.

Chang, C.-R., Li, M.-H., Chang, S.-D., 2007. A preliminary study on the local cool-island intensity of Taipei City parks. Landsc. Urban Plan. 80, 386–395.

Coutts, A.M., Tapper, N.J., Beringer, J., Loughnan, M., Demuzere, M., 2013. Watering our cities: the capacity for water sensitive urban design to support urban cooling and improve human thermal comfort in the Australian context. Prog. Phys. Geogr. 37, 2–28.

Currie, B.A., Bass, B., 2008. Estimates of air pollution mitigation with green plants and green roofs using the ufore model. Urban Ecosyst. 11, 409–422.

Daniel, M., Lemonsu, A., Viguié, V., 2016. Role of watering practices in large-scale urban planning strategies to face the heat-wave risk in future climate. Urban Climate.

de Munck, C., 2013. Modélisation de la végétation urbaine et stratégies d'adaptation pour l'amélioration du confort climatique et de la demande énergetique en ville. INPT, Institut National Polytechnique de Toulouse, France. Ph.D. thesis. http://ethesis.inp-toulouse.fr/archive/00002485/.

de Munck, C., Lemonsu, A., Bouzouidja, R., Masson, V., Claverie, R., 2013a. The GREENROOF module (v7. 3) for modelling green roof hydrological and energetic performances within TEB. Geosci. Model Dev. 6, 1941–1960.

de Munck, C., Pigeon, G., Masson, V., Meunier, F., Bousquet, P., Tréméac, B., Merchat, M., Poeuf, P., Marchadier, C., 2013b. How much can air conditioning increase air temperatures for a city like Paris, France? Int. J. Climatol. 33, 210–227. http://ethesis.inp-toulouse.fr/archive/00002485/.

Département du Val de Marne, 2016. Le réseau parisien d'eau non potable, une alternative a l'eau potable pleine de ressource. http://www.valdemarne.fr/newsletters/plan-bleu-du-val-de-marne/le-reseau-parisien-deau-non-potable-une-alternative-a-leau-potable-pleine-de-ressource.

Doukari, O., Aguejdad, R., Houet, T., 2016. SLEUTH*: un modéle d'expansion urbaine pour une approche scénario–dépendante". Revue Internationale de Géomatique 26 (1), 7–32.

Dousset, B., Gourmelon, F., Laaidi, K., Zeghnoun, A., Giraudet, E., Bretin, P., Mauri, E., Vandentorren, S., 2011. Satellite monitoring of summer heat waves in the Paris metropolitan area. Int. J. Climatol. 31, 313–323.
Eumorfopoulou, E., Aravantinos, D., 1998. The contribution of a planted roof to the thermal protection of buildings in Greece. Energy Build. 27, 29–36.
Eumorfopoulou, E., Kontoleon, K., 2009. Experimental approach to the contribution of plant-covered walls to the thermal behaviour of building envelopes. Energy Build. 44, 1024–1038.
Fiala, D., Havenith, G., Bröde, P., Kampmann, B., Jendritzky, G., 2012. Utci-fiala multi-node model of human heat transfer and temperature regulation. Int. J. Biometeorol. 56, 429–441.
Getter, K.L., Rowe, D.B., 2006. The role of extensive green roofs in sustainable development. HortScience 41, 1276–1285.
Giorgi, F., 2006. Climate change hot-spots. Geophys. Res. Lett. 33, ISSN 1944-8007. http://dx.doi.org/10.1029/2006GL025734. n/a–n/a.
Groupe Descartes, 2009. Consultation internationale de recherche et de développement sur le Grand Pari de l'agglomération parisienne. Rapport Final. http://www.legrandparis.net/actualitedetail/82/DESCARTES_Livret_chantier_1_2.pdf.
Hamdi, R., Masson, V., 2008. Inclusion of a drag approach in the Town Energy Balance (TEB) scheme: offline 1D evaluation in a street canyon. J. Appl. Meteorol. Climatol. 47, 2627–2644.
Hémon, D., Jougla, E., 2004. Surmortalité liée à la canicule d'août 2003. Rapport remis au Ministre de la Santé et de la protection sociale. 26 octobre 2004. Technical Report. Institut National de la santé et de la recherche médicale. http://www.inserm.fr/content/download/1435/13095/file/canicule_octobre2004.pdf.
Hill, A.C., 1971. Vegetation: a sink for atmospheric pollutants. J. Air Pollut. Control Assoc. 21, 341–346.
Kontoleon, K., Eumorfopoulou, E., 2010. The effect of the orientation and proportion of a plant-covered wall layer on the thermal performance of a building zone. Build. Environ. 45, 1287–1303.
Kounkou-Arnaud, R., Desplat, J., Lemonsu, A., Salagnac, J., 2013. Epicea: étude des impacts du changement climatique à paris. La Météorologie 84, 42–48.
Le Bras, J., Masson, V., 2015. A fast and spatialized urban weather generator for long-term urban studies at the city-scale. Front. Earth Sci. 3, 27.
Ledrans, M., Vandentorren, S., Bretin, P., Croisier, A., 2005. Étude des facteurs de risque de décès des personnes âgées résidant à domicile durant la vague de chaleur d'août 2003. Rapport de l'Institut national de Veille Sanitaire. pp. 1–116.
Lemonsu, A., Kounkou-Arnaud, R., Desplat, J., Salagnac, J.-L., Masson, V., 2013. Evolution of the parisian urban climate under a global changing climate. Clim. Chang. 116, 679–692.
Lemonsu, A., Masson, V., Berthier, E., 2007. Improvement of the hydrological component of an urban soil-vegetation-atmosphere-transfer model. Hydrocarb. Process. 21, 2100–2111.
Lemonsu, A., Masson, V., Shashua-Bar, L., Erell, E., Pearlmutter, D., 2012. Inclusion of vegetation in the Town Energy Balance model for modelling urban green areas. Geosci. Model Dev. 5, 1377–1393.
Lemonsu, A., Viguié, V., Daniel, M., Masson, V., 2015. Vulnerability to heat waves: impact of urban expansion scenarios on urban heat island and heat stress in Paris (France). Urban Climate 14, 586–605.
Liangmei, H., Jianlong, L., Dehua, Z., Jiyu, Z., 2008. A fieldwork study on the diurnal changes of urban microclimate in four types of ground cover and urban heat island of Nanjing, China. Build. Environ. 43, 7–17. http://dx.doi.org/10.1016/j.buildenv.2006.11.025.
Madre, F., Vergnes, A., Machon, N., Clergeau, P., 2014. Green roofs as habitats for wild plant species in urban landscapes: first insights from a large-scale sampling. Landsc. Urban Plan. 122, 100–107.
Marchadier, C., 2013. Construction des scénarios MUSCADE. Bâti, technologies et usages. Rapport de projet. Mars 2013.
Masson, V., 2000. A physically-based scheme for the urban energy budget in atmospheric models. Bound.-Lay. Meteorol. 94, 357–397.
Masson, V., Marchadier, C., Adolphe, L., Aguejdad, R., Avner, P., Bonhomme, M., Bretagne, G., Briottet, X., Bueno, B., de Munck, C., et al. 2014a. Adapting cities to climate change: a systemic modelling approach. Urban Climate 10, 407–429.
Masson, V., Moigne, P.L., Martin, E., Faroux, S., Alias, A., Alkama, R., Belamari, S., Barbu, A., Boone, A., Bouyssel, F., et al. 2013. The SURFEX v7.2 land and ocean surface platform for coupled or offline simulation of earth surface variables and fluxes. Geosci. Model Dev. 6, 929–960.
Masson, V., Pigeon, G., Lemonsu, A., Marchadier, C., Hidalgo, J., Bueno, B., de Munck, C., Daniel, M., Viguié, V., Genovese, E., Salagnac, J.-L., Zibouche, K., Long, N., Levellier, T., Bonhomme, M., Ait-Haddou, H., Adolphe, L., Faraut, S., Nolorgues, L., 2014b. Modélisation urbaine et stratégies d'adaptation au changement climatique pour anticiper la demande et la production énergétique (Muscade). Projet ANR-09-VILL-0003. Programme Ville Durable 2009. Rapport final, 2014. http://www.cnrm-gamemeteo.fr/ville.climat/IMG/pdf/muscade_rapportfinal.pdf.
Masson, V., Seity, Y., 2009. Including atmospheric layers in vegetation and urban offline surface schemes. J. Appl. Meteorol. Climatol. 48, 1377–1397.
Meehl, G.A., Tebaldi, C., 2004. More intense, more frequent, and longer lasting heat waves in the 21st century. Science 305, 994–997. http://science.sciencemag.org/content/305/5686/994.full.pdf.
Mullaney, J., Lucke, T., Trueman, S.J., 2015. A review of benefits and challenges in growing street trees in paved urban environments. Landsc. Urban Plan. 134, 157–166.
Ng, E., Chen, L., Wang, Y., Yuan, C., 2012. A study on the cooling effects of greening in a high-density city: an experience from Hong Kong. Build. Environ. 47, 256–271.
Noilhan, J., Mahfouf, J., 1996. The ISBA land surface parameterisation scheme. Glob. Planet. Chang. 13, 145–159.
Nowak, D.J., Crane, D.E., Stevens, J.C., 2006. Air pollution removal by urban trees and shrubs in the United States. Urban For. Urban Green. 4, 115–123.
Onmura, S., Matsumoto, M., Hokoi, S., 2001. Study on evaporative cooling effect of roof lawn gardens. Energ. Buildings 33, 653–666.
Pigeon, G., 2011. Computation of a thermal comfort index in the TEB urban canopy model. Technical Report for the VURCA Project, ANR-08-VULN-013-0x/VURCA.
Pigeon, G., Zibouche, K., Bueno, B., Le Bras, J., Masson, V., 2014. Improving the capabilities of the town energy balance model with up-to-date building energy simulation algorithms: an application to a set of representative buildings in Paris. Energ. Buildings 76, 1–14.
Plazzotta, M., 2015. Adaptation des villes au changement climatique. rapport de stage de master. 2 fvrier 2015 15 juin 2015. Technical Report. Universit Paul Sabatier, Toulouse III, France.
Potchter, O., Cohen, P., Bitan, A., 2006. Climatic behavior of various urban parks during hot and humid summer in the Mediterranean city of Tel Aviv, Israel. Int. J. Climatol. 26, 1695–1711.
Pugh, T.A., MacKenzie, A.R., Whyatt, J.D., Hewitt, C.N., 2012. Effectiveness of green infrastructure for improvement of air quality in urban street canyons. Environ. Sci. Technol. 46, 7692–7699.
Redon, E., Lemonsu, A., Masson, V., Morille, B., Musy, M., 2016. Implementation of street trees within the solar radiative exchange parameterization of TEB in SURFEX v8.0. GMD.
Rosenzweig, C., Solecki, W.D., Parshall, L., Lynn, B., Cox, J., Goldberg, R., Hodges, S., Gaffin, S., Slosberg, R.B., Savio, P., et al. 2009. Mitigating New York City's heat island. Bull. Am. Meteorol. Soc. 90, 1297–1312.
RTE [Réseau de transport d'électricité], 2016. Bilan électrique 2015 et perspectives en région ILE-DE-FRANCE. http://www.rte-france.com/sites/default/files/2016_12_05_bilan_electrique_ile-de-france.pdf.
Shashua-Bar, L., Hoffman, M., 2000. Vegetation as a climatic component in the design of an urban street. An empirical model for predicting the cooling effect of urban green areas with trees. Energ. Buildings 31, 221–235.
Shashua-Bar, L., Pearlmutter, D., Erell, E., 2009. The cooling efficiency of urban landscape strategies in a hot dry climate. Landsc. Urban Plan. 92, 179–186.
SOPREMA, 2011. Fiche générale d'arrosage des systmes SOPRANATURE, Version03032011. http://www.soprema.fr/actualites/nouveaux-produits/1383/1330753/Aquatex-nouvelle-solution-d-irrigation-raisonnee.
Souch, C., Souch, C., 1993. The effect of trees on summertime below canopy urban climates: a case study Bloomington, Indiana. J. Arboricult. 19, 303–312.
Sternberg, T., Viles, H., Cathersides, A., 2011. Evaluating the role of ivy (*Hedera helix*) in moderating wall surface microclimates and contributing to the bioprotection of historic buildings. Build. Environ. 46, 293–297.

Stocker, T., Qin, D., Plattner, G.-K., Alexander, L., Allen, S., Bindoff, N., Breon, F.-M., Church, J., Cubasch, U., Emori, S., Forster, P., Friedlingstein, P., Gillett, N., Gregory, J., Hartmann, D., Jansen, E., Kirtman, B., Knutti, R., KrishnaKumar, K., Lemke, P., Marotzke, J., Masson-Delmotte, V., Meehl, G., Mokhov, I., Piao, S., Ramaswamy, V., Randall, D., Rhein, M., Rojas, M., Sabine, C., Shindell, D., Talley, L., 2013. Technical Summary. Climate Change 2013: The Physical Science Basis. Contribution of Working Group I to the Fifth Assessment Report of the Intergovernmental Panel on Climate Change. Cambridge University Press, Cambridge, United Kingdom and New York, NY, USA, pp. 33115. book section. http://dx.doi.org/10.1017/CBO9781107415324.005.

Stovin, V., 2010. The potential of green roofs to manage urban stormwater. Water Environ. J. 24, 192–199.

Stovin, V., Jorgensen, A., Clayden, A., 2008. Street trees and stormwater management. Arbitr. J. 30, 297–310.

Taha, H., Akbari, H., Rosenfeld, A., 1991. Heat island and oasis effects of vegetative canopies: micro-meteorological field-measurements. Theor. Appl. Climatol. 44, 123–138.

Takebayashi, H., Moriyama, M., 2007. Surface heat budget on green roof and high reflection roof for mitigation of urban heat island. Build. Environ. 42, 2971–2979.

The Commission for Thermal Physiology of the International Union of Physiological Sciences, 2003. Glossary of terms for thermal physiology. J. Theor. Biol. 28, 75–106.

Viguié, V., Hallegatte, S., 2012. Trade-offs and synergies in urban climate policies. Nat. Clim. Chang. 2, 334–337.

Viguié, V., Hallegatte, S., Rozenberg, J., 2014. Downscaling long term socio-economic scenarios at city scale: a case study on Paris. Technol. Forecast. Soc. Chang. 87, 305–324.

Wikipedia, 2015. Débit de la seine à Paris. https://fr.wikipedia.org/wiki/Debit_de_la_Seine_a_Paris.

Wong, N.H., Kwang Tan, A.Y., Chen, Y., Sekar, K., Tan, P.Y., Chan, D., Chiang, K., Wong, N.C., 2010. Thermal evaluation of vertical greenery systems for building walls. Build. Environ. 45, 663–672.